ELSEVIER

Coordination Chemistry Reviews 144 (1995) 287–319

COORDINATION CHEMISTRY REVIEWS

Intramolecular equilibria in metal ion complexes of artificial nucleotide analogues with antiviral properties. A case study

Helmut Sigel

Institute of Inorganic Chemistry, University of Basel, Spitalstrasse 51, CH-4056 Basel, Switzerland

Received 14 October 1994

Contents

Abstract

The stability constants of the 1:1 complexes formed between Mg^{2+}, Ca^{2+}, Sr^{2+}, Ba^{2+}, Mn^{2+}, Co^{2+}, Ni^{2+}, Cu^{2+}, Zn^{2+}, or Cd^{2+} and (phosphonomethoxy)ethane (PME^{2-}) or

SSDI 0010-8545(95)01158-7

9-[2-(phosphonomethoxy)ethyl]adenine ($PMEA^{2-}$), an adenosine monophosphate (AMP^{2-}) analogue, are used in combination with $\log K^{M}_{M(R\text{-}PO_3)}$ versus $pK^{H}_{H(R\text{-}PO_3)}$ straight-line plots (where R in $R\text{–}PO_3^{2-}$ is a non-coordinating residue) to demonstrate that for all the M(PME) and M(PMEA) complexes with the mentioned metal ions a stability higher than expected for a sole phosphonate coordination of the metal ion occurs. This increased stability is due to the formation of five-membered chelates involving the ether oxygen present in the $\text{–O–CH}_2\text{–PO}_3^{2-}$ residue of PME^{2-}; the same is true to a large extent also for the M(PMEA) complexes. However, e.g., for the complex formed between Cu^{2+} and $PMEA^{2-}$ an *additional* stability increase is observed which has to be attributed to a metal ion–adenine interaction thus giving rise to equilibria between three different M(PMEA) isomers. A procedure, which is generally applicable, for the analysis of such intramolecular equilibria is summarized. For Cu(PMEA) it is calculated that 17 (±3)% exist as an isomer with a sole Cu^{2+}–phosphonate coordination, 34 (±10)% form the mentioned five-membered chelate involving the ether oxygen, and the remaining 49 (±10)% are due to an isomer, designated $Cu(PMEA)_{cl/Ad}$, which also contains a Cu^{2+}–adenine interaction. Based on various arguments it is suggested that this latter isomer probably contains two chelate rings which result from a metal ion coordination to the phosphonate group, the ether oxygen, and N-3 of the adenine residue. Interestingly, the formation degree of $Cu(PMEA)_{cl/Ad}$ passes through a minimum upon addition of 1,4-dioxane to the aqueous solution; i.e., small amounts of dioxane inhibit the Cu^{2+}–adenine interaction, while larger amounts favor it again. This solvent effect is analogous to an observation made with the macrochelate of Cu(5′-AMP) in which the metal ion is bound to the phosphate group and N-7 of the adenine residue. Moreover, ternary Cu(arm)(PMEA) systems, where arm = 2,2′-bipyridyl (bpy) or 1,10-phenanthroline (phen), are analyzed. It is shown that also in these systems three isomeric species form intramolecular equilibria; e.g., of Cu(bpy)(PMEA) about 3% exist with the metal ion solely coordinated to the phosphonate group, 10% as a five-membered chelate involving the $\text{–O–CH}_2\text{–PO}_3^{2-}$ residue of $PMEA^{2-}$, and 87% with an intramolecular stack between the adenine moiety of $PMEA^{2-}$ and the aromatic rings of bpy. Finally, the properties of $PMEA^{2-}$ and 5′-AMP^{2-} are compared, and it is emphasized that the ether oxygen, which influences the stability and especially the structure of the M(PMEA) complexes in solution, is crucial for the antiviral properties of PMEA. The properties of a related compound, i.e., (*S*)-9-[3-hydroxy-2-(phosphonomethoxy)-propyl]adenine ($HPMPA^{2-}$), which differs from $PMEA^{2-}$ by the additional presence of a $\text{–CH}_2\text{OH}$ group in the chain bound to the adenine moiety, i.e., in the $\text{–CH}_2\text{–CH(CH}_2\text{OH)–O–CH}_2\text{–PO}_3^{2-}$ residue, are also shortly indicated and some general aspects of enzymic reactions with nucleotides are considered.

Keywords: Intramolecular equilibria; Metal ion complexes; Antiviral nucleotide analogues; Nucleotide complexes; Adenoside monophosphate analogues

Abbreviations

2′-AMP^{2-}	adenosine 2′-monophosphate
3′-AMP^{2-}	adenosine 3′-monophosphate
5′-AMP^{2-}	adenosine 5′-monophosphate
arm	heteroaromatic nitrogen base (e.g., bpy or phen)
bpy	2,2′-bipyridyl
DNA	deoxyribonucleic acid

$HPMPA^{2-}$	dianion of (*S*)-9-[3-hydroxy-2-(phosphonomethoxy)propyl]adenine
M^{2+}	divalent metal ion
NMR	nuclear magnetic resonance
phen	1,10-phenanthroline
PME^{2-}	dianion of (phosphonomethoxy)ethane (=ethoxymethanephosphonate)
$PMEA^{2-}$	dianion of 9-[2-(phosphonomethoxy)ethyl]adenine
RNA	ribonucleic acid
$R\text{-}PO_3^{2-}$	general phosphonate and (in part also) general phosphate monoester ligand

1. Introduction

Considering that nucleotides play a key role in many metabolic processes it is not surprising that a large number of nucleotide analogues have been synthesized with the aim of obtaining therapeutically usable agents [1–4]. One of the difficulties is that base- or sugar-modified nucleotide analogues with phosphate ester residues are known to undergo enzyme-catalyzed dephosphorylation during their passage through the cellular membrane or in blood plasma [3]. This undesired biological reaction renders therapeutic application of such antimetabolites inefficient. This difficulty may be circumvented by applying nucleotide analogues with a phosphonate residue [3].

The AMP analogue 9-[2-(phosphonomethoxy)ethyl]adenine (PMEA; see Fig. 1) shows antiviral properties [4] (see also Section 10). This phosphonate derivative is converted by cellular nucleotide kinases into its diphosphate, which may be considered a triphosphate analogue, and as such it inhibits viral and to a lesser extent, cellular DNA synthesis [4,5]. Considering that DNA and RNA polymerases in general also depend on the presence of metal ions [6], mostly Mg^{2+} and Zn^{2+}, it is appealing to study the metal ion binding properties of PMEA and related phosphonates [7–12].

Inspection of the structure of the dianion of PMEA (=$PMEA^{2-}$) shown in Fig. 1 [13,14] indicates that $PMEA^{2-}$ should be an interesting ambivalent ligand [15] which justifies detailed studies also from a coordination chemical point of view. Indeed, this ligand allows a demonstration of how equilibria between various isomeric complexes may be treated. As a case study, the basic reasonings for such a treatment are outlined below; evidently, a corresponding treatment may also be applied to other isomeric equilibria.

2. Possible isomers of binary metal ion–$PMEA^{2-}$ complexes

From Fig. 1 it is evident that $PMEA^{2-}$ offers to metal ions the 2-fold negatively charged phosphonate group for binding and based on the experience with nucleotides [16–18] one may assume — and indeed this is proven in Section 5 (Fig. 2, vide

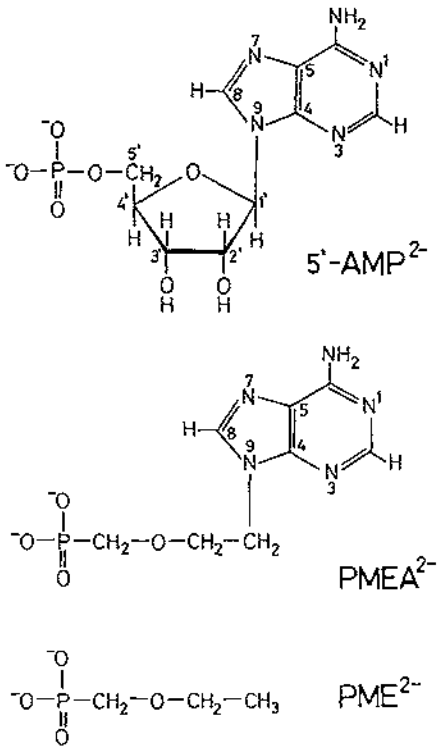

Fig. 1. Chemical structure of the dianion of 9-[2-(phosphonomethoxy)ethyl]adenine ($PMEA^{2-}$) in comparison with the structures of adenosine 5'-monophosphate (5'-AMP^{2-}), which is shown in its dominating *anti* conformation [13,14], and the dianion of (phosphonomethoxy)ethane (PME^{2-} = ethoxymethanephosphonate).

infra) — that this group is the primary binding site which largely determines the overall stability of M(PMEA) complexes, where $M^{2+} = Mg^{2+}$, Ca^{2+}, Sr^{2+}, Ba^{2+}, Mn^{2+}, Co^{2+}, Ni^{2+}, Cu^{2+}, Zn^{2+}, or Cd^{2+}. The next potential binding site is the ether oxygen in the $-CH_2-O-CH_2-PO_3^{2-}$ residue because earlier studies [19] on different ligand systems have shown that the ether oxygen may bind to the mentioned divalent metal ions provided it is suitably oriented toward a primary binding site allowing the formation of chelates. Indeed, it is also apparent from Fig. 1 that a metal ion coordinated to the phosphonate group may form a five-membered chelate involving the ether oxygen. Hence, the following equilibrium (1) needs to be considered:

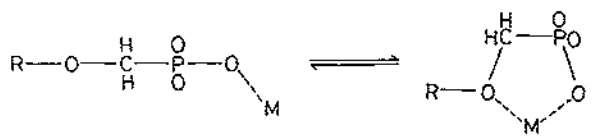

(1)

The potential binding sites for metal ions at the adenine residue are N-1, N-3, and

N-7. The N-1 site is of no further concern because it cannot be reached by a metal ion already bound at the phosphonate group. With N-7 a macrochelate may be formed via the interaction of a metal ion already bound to the phosphonate group; in fact, the corresponding situation is well known for complexes of purine-nucleoside 5′-monophosphates [16,20–22]. Finally, N-3 needs to be considered and indeed, molecular models reveal that a metal ion chelated to the phosphonate and the ether O-atom may further interact with N-3 by forming a seven-membered chelate. It may be emphasized that the formation of a macrochelate involving only the phosphonate group and N-3 is highly unlikely because its formation would force the ether atom into the coordination sphere of the metal ion [7,9].

The above reasonings lead to the following two equilibrium schemes. In the first case (Eq. (2))

$$M^{2+} + PMEA^{2-} \overset{K^{M}_{M(PMEA)_{op}}}{\rightleftharpoons} M(PMEA)_{op} \begin{cases} \overset{K_{I/O}}{\rightleftharpoons} M(PMEA)_{cl/O} \\ \overset{K_{I/N7}}{\rightleftharpoons} M(PMEA)_{cl/N7} \end{cases} \quad (2)$$

the metal ion binds initially to the phosphonate group giving rise to an 'open' species, which is designated $M(PMEA)_{op}$ and which may transfer either into $M(PMEA)_{cl/O}$, i.e., into the five-membered chelate involving the ether O-atom (Eq. (1)), or into a macrochelate involving N-7, designated $M(PMEA)_{cl/N7}$. A *simultaneous* binding of a phosphonate-bound metal ion to the ether O-atom *and* to N-7 is for steric reasons not possible. The second scheme (Eq. (3)) consists of successive equilibria:

$$M^{2+} + PMEA^{2-} \overset{K^{M}_{M(PMEA)_{op}}}{\rightleftharpoons} M(PMEA)_{op} \overset{K_{I/O}}{\rightleftharpoons} M(PMEA)_{cl/O} \overset{K_{I/O/N3}}{\rightleftharpoons} M(PMEA)_{cl/O/N3} \quad (3)$$

At first the phosphonate-coordinated isomer, $M(PMEA)_{op}$, forms the five-membered chelate with the ether O-atom and next the 2-fold chelated species involving also N-3, designated $M(PMEA)_{cl/O/N3}$, is created.

Both equilibrium schemes (2) and (3) have in common that they contain three isomeric species. In order to see whether $M(PMEA)_{cl/N7}$ and/or $M(PMEA)_{cl/O/N3}$ are of any relevance the metal ion-binding properties of (phosphonomethoxy)ethane (= PME^{2-} = ethoxymethanephosphonate; see Fig. 1) may be considered. It is evident that equilibrium (1) also applies to this ligand as well as those parts of the equilibrium schemes (2) and (3) which do not involve the adenine moiety; in other words, studies with PME^{2-} will reveal the effect of the adenine moiety on the stability of M(PMEA) complexes.

3. Considerations on the stability and formation degree of $M(PME)_{cl}$ and $M(PMEA)_{cl/O}$ complexes

As indicated above, equilibrium (1) is part of both equilibrium schemes (2) and (3); therefore, it will be considered first. The position of this concentration-independent

equilibrium (1) between an 'open' isomer, $M(PME)_{op}$ or $M(PMEA)_{op}$, and a 'closed' species involving the ether-O atom, $M(PME)_{cl}$ or $M(PMEA)_{cl/O}$ (see also Fig. 1), is defined by the intramolecular and, hence, dimension-less equilibrium constant K_I:

$$K_I = [M(PME)_{cl}]/[M(PME)_{op}] \tag{4}$$

In Eq. (4), as well as in the following Eqs. (5)–(13), M(PME), $M(PME)_{op}$ and $M(PME)_{cl}$ may always be replaced by M(PMEA), $M(PMEA)_{op}$ and $M(PMEA)_{cl/O}$, respectively. This means PME^{2-} is employed here for reasons of simplicity but all derivations and conclusions hold for both ligands, i.e. PME^{2-} and $PMEA^{2-}$, as long as only equilibrium (1) is operating for $PMEA^{2-}$ also.

Generally, the stability constants of 1:1 complexes measured experimentally are defined in analogy to Eq. (5):

$$M^{2+} + PME^{2-} \rightleftharpoons M(PME) \tag{5a}$$

$$K^{M}_{M(PME)} = [M(PME)]/([M^{2+}][PME^{2-}]) \tag{5b}$$

This means that [M(PME)] represents the sum of the concentrations of all M(PME) isomers present. Clearly, due to equilibrium (1) the expressions (5) may therefore be rewritten as given in Eqs. (6) and (7),

$$M^{2+} + PME^{2-} \rightleftharpoons M(PME)_{op} \rightleftharpoons M(PME)_{cl} \tag{6}$$

$$K^{M}_{M(PME)} = \frac{([M(PME)_{op}] + [M(PME)_{cl}]}{[M^{2+}][PME^{2-}]} = \frac{[M(PME)_{op}]}{[M^{2+}][PME^{2-}]} + \frac{[M(PME)_{cl}]}{[M^{2+}][PME^{2-}]} \tag{7}$$

and then further developed [19,20] to Eqs. (8) and (9):

$$K^{M}_{M(PME)} = K^{M}_{M(PME)_{op}} + K_I \cdot K^{M}_{M(PME)_{op}} \tag{8a}$$

$$= K^{M}_{M(PME)_{op}}(1 + K_I) \tag{8b}$$

$$K_I = \frac{K^{M}_{M(PME)}}{K^{M}_{M(PME)_{op}}} - 1 = 10^{\log\Delta} - 1 \tag{9}$$

The stability constant of the open isomer, $K^{M}_{M(PME)_{op}}$ (Eq. (10)),

$$K^{M}_{M(PME)_{op}} = [M(PME)_{op}]/([M^{2+}][PME^{2-}]) \tag{10}$$

is not directly accessible by experiments, yet it may be calculated with the measureable acidity constant, $K^{H}_{H(PME)}$ (Eq. (11)),

$$K^{H}_{H(PME)} = [H^{+}][PME^{2-}]/[H(PME)^{-}] \tag{11}$$

which is due to the deprotonation of the $-P(O)_2(OH)^{-}$ residue in $H(PME)^{-}$, and the equations of the correlation lines for $\log K^{M}_{M(R\text{-}PO_3)}$ versus $pK^{H}_{H(R\text{-}PO_3)}$ plots (where $R\text{–}PO_3^{2-}$ represents simple phosphonate or phosphate monoester ligands with a non-coordinating residue R) as listed in Table 1 [7,23] for the ten metal ions already mentioned. As one would expect, the equilibrium data for the simple methane-

Table 1
Straight-line correlations for M^{2+}–phosphonate or phosphate complex stabilities and phosphonate or phosphate group basicities (25 °C; I = 0.1 M, $NaNO_3$)[a,b]

M^{2+}	m	b	SD
Mg^{2+}	0.208 ± 0.015	0.272 ± 0.097	0.033
Ca^{2+}	0.131 ± 0.020	0.636 ± 0.131	0.048
Sr^{2+}	0.082 ± 0.016	0.732 ± 0.102	0.036
Ba^{2+}	0.087 ± 0.016	0.622 ± 0.107	0.039
Mn^{2+}	0.238 ± 0.022	0.683 ± 0.144	0.051
Co^{2+}	0.223 ± 0.026	0.554 ± 0.167	0.057
Ni^{2+}	0.245 ± 0.023	0.422 ± 0.147	0.051
Cu^{2+}	0.465 ± 0.025	−0.015 ± 0.164	0.057
Zn^{2+}	0.345 ± 0.026	−0.017 ± 0.171	0.060
Cd^{2+}	0.329 ± 0.019	0.399 ± 0.127	0.045

[a] The slopes (m) and intercepts (b) for the straight base lines from plots of log $K^{M}_{M(R\text{-}PO_3)}$ versus $pK^{H}_{H(R\text{-}PO_3)}$ were calculated [7] from the equilibrium constants determined earlier for six simple phosphate monoesters (4-nitrophenyl phosphate, phenyl phosphate, *n*-butyl phosphate, D-ribose 5-monophosphate, uridine 5′-monophosphate, and thymidine 5′-monophosphate) [23] and two simple phosphonates (methanephosphonate and ethanephosphonate) [7]. The column at the right lists 3-times the standard deviations (SD) resulting from the differences between the experimental and calculated values for the mentioned eight ligand systems.

[b] The above data are abstracted from Tables 5 and 6 in Ref. [7]. Straight-line equation: $y = m \cdot x + b$, where x represents the pK_a value of any phosphate monoester or phosphonate ligand and y the calculated stability constant (log$K$) of the corresponding $M(R\text{–}PO_3)$ complex; the errors given with m and b correspond to 1 standard deviation (1σ). The listed SD values (column at the right; 3σ) are considered as reasonable error limits for any stability constant calculation in the pK_a range 5 to 8.

phosphonate and ethanephosphonate ligands also fit on these straight lines (see also Fig. 2, vide infra). Hence, with this procedure log $K^{M}_{M(PME)_{op}}$ is obtained and thus the stability-constant difference of Eq. (12)

$$\log \Delta = \log \Delta_{M(PME)} = \log K^{M}_{M(PME)_{exper}} - \log K^{M}_{M(PME)_{calc}} \quad (12a)$$

$$= \log K^{M}_{M(PME)} - \log K^{M}_{M(PME)_{op}} = \log (1 + E) \quad (12b)$$

can be calculated, which then also defines the second term in the above Eq. (9). It may be added that the value for $10^{\log \Delta}$ is sometimes also addressed as the stability enhancement factor $(1 + E)$ [19].

Clearly, the reliability of any calculation for K_I (Eqs. (4) and (9)) depends on the accuracy of the difference log $\Delta_{M(PME)}$ which becomes the more important the more similar the two constants in Eq. (12b) are. Therefore, only well-defined error limits allow a quantitative evaluation of the position of equilibrium (1). Finally, if K_I is known, the percentage of the closed or chelated species occurring in equilibrium (1) follows from Eq. (13).

$$\%M(PME)_{cl} = 100 \cdot K_I/(1 + K_I) \quad (13)$$

Application of this procedure [19,20] yields the results listed in Tables 2 and 3 (vide infra) which will be discussed in Section 5.

4. Evaluation procedure for the three-isomer problem of the M(PMEA) complexes

Three-isomer equilibria have so far rarely been treated in the literature (see e.g. Refs. [7,24]). Assuming that aside from the $M(PMEA)_{op}$ and $M(PMEA)_{cl/O}$ species considered in Section 3 additional isomers as summarized in the equilibrium schemes (2) and (3) occur, their formation must be recognizable by a further stability increase which goes beyond the one connected with equilibrium (1). This case will now be considered.

Application of the mass action law to the equilibrium scheme (2) leads to the definitions (14)–(16):

$$\log K^{M}_{M(PMEA)_{op}} = [M(PMEA)_{op}]/([M^{2+}][PMEA^{2-}]) \tag{14}$$

$$K_{I/O} = [M(PMEA)_{cl/O}]/[M(PMEA)_{op}] \tag{15}$$

$$K_{I/N7} = [M(PMEA)_{cl/N7}]/[M(PMEA)_{op}] \tag{16}$$

Of course, the experimentally accessible overall stability constant as defined in Eq. (17a) may then be rewritten as given in the expressions (17b), (17c), and (17d):

$$K^{M}_{M(PMEA)} = \frac{[M(PMEA)]}{[M^{2+}][PMEA^{2-}]} \tag{17a}$$

$$= \frac{([M(PMEA)_{op}] + [M(PMEA)_{cl/O}] + [M(PMEA)_{cl/N7}])}{[M^{2+}][PMEA^{2-}]} \tag{17b}$$

$$= K^{M}_{M(PMEA)_{op}} + K_{I/O} \cdot K^{M}_{M(PMEA)_{op}} + K_{I/N7} \cdot K^{M}_{M(PMEA)_{op}} \tag{17c}$$

$$= K^{M}_{M(PMEA)_{op}}(1 + K_{I/O} + K_{I/N7}) \tag{17d}$$

Based on Eqs. (14), (15), and (18) the corresponding derivation is obtained for the equilibrium scheme (3):

$$K_{I/O/N3} = [M(PMEA)_{cl/O/N3}]/[M(PMEA)_{cl/O}] \tag{18}$$

$$K^{M}_{M(PMEA)} = \frac{[M(PMEA)]}{[M^{2+}][PMEA^{2-}]} \tag{19a}$$

$$= \frac{([M(PMEA)_{op}] + [M(PMEA)_{cl/O}] + [M(PMEA)_{cl/O/N3}])}{[M^{2+}][PMEA^{2-}]} \tag{19b}$$

$$= K^{M}_{M(PMEA)_{op}} + K_{I/O} \cdot K^{M}_{M(PMEA)_{op}} + K_{I/O} \cdot K_{I/O/N3} \cdot K^{M}_{M(PMEA)_{op}} \tag{19c}$$

$$= K^{M}_{M(PMEA)_{op}}(1 + K_{I/O} + K_{I/O} \cdot K_{I/O/N3}) \tag{19d}$$

It is apparent that Eqs. (17d) and (19d) transfer into $K^{M}_{M(PMEA)} = K^{M}_{M(PMEA)_{op}}$ if no five-membered chelates are formed and if no interaction with the adenine moiety occurs. For the case that only no interaction with the adenine residue takes place, i.e., $M(PMEA)_{cl/N7}$ and/or $M(PMEA)_{cl/O/N3}$ are not formed, the equilibrium schemes (2) and (3) reduce to equilibrium (1); in other words, to the situation also possible with PME^{2-} (cf. Fig. 1). The corresponding definitions have been given in Section 3

in Eqs. (4), (7), and (8). Considering further that $M(PME)_{cl}$ and $M(PMEA)_{cl/O}$ correspond to each other regarding the structures of the chelates, it is evident that in the case that no adenine-bound isomers are formed, Eqs. (17d) and (19d) reduce to Eq. (8b).

In analogy to Eqs. (4) and (9) in Section 3 and based on Eq. (17d) one arrives easily [7,24] at the following Eq. (20):

$$K_I = K_{I/tot} = \frac{K^M_{M(PMEA)}}{K^M_{M(PMEA)_{op}}} - 1 = 10^{\log\Delta} - 1 \tag{20a}$$

$$= \frac{[M(PMEA)_{cl/tot}]}{[M(PMEA)_{op}]} = \frac{([M(PMEA)_{cl/O}] + [M(PMEA)_{cl/N7}])}{[M(PMEA)_{op}]} \tag{20b}$$

$$= K_{I/O} + K_{I/N7} \tag{20c}$$

Similarly, based on Eq. (19d), follows Eq. (21):

$$K_I = K_{I/tot} = \frac{K^M_{M(PMEA)}}{K^M_{M(PMEA)_{op}}} - 1 = 10^{\log\Delta} - 1 \tag{21a}$$

$$= \frac{[M(PMEA)_{cl/tot}]}{[M(PMEA)_{op}]} = \frac{([M(PMEA)_{cl/O}] + [M(PMEA)_{cl/O/N3}])}{[M(PMEA)_{op}]} \tag{21b}$$

$$= K_{I/O} + K_{I/O} \cdot K_{I/O/N3} = K_{I/O}(1 + K_{I/O/N3}) \tag{21c}$$

Clearly, it is again evident that if the second 'closed' isomer, $M(PMEA)_{cl/N7}$ or $M(PMEA)_{cl/O/N3}$, is not formed, the above Eqs. (20c) and (21c) reduce to the two-isomer problem (Eq. (1)) treated in Eq. (9). It should be noted further that the differences between Eqs. (20c) and (21c) originate in the different order of the successive equilibria in schemes (2) and (3). This leads then to different definitions for some of the intramolecular equilibria (Eqs. (16) and (18)), and hence to different dependencies of K_I, i.e. $K_{I/tot}$ (see Eqs. (20c) and (21c)).

Values for K_I ($= K_{I/tot}$) can be calculated according to Eqs. (20c) or (21c), because in analogy to Eq. (12) the observed stability increase, if schemes (2) and/or (3) are operating, is defined by Eq. (22):

$$\log\Delta = \log\Delta_{M(PMEA)} = \log K^M_{M(PMEA)_{exper}} - \log K^M_{M(PMEA)_{calc}} \tag{22a}$$

$$= \log K^M_{M(PMEA)} - \log K^M_{M(PMEA)_{op}} \tag{22b}$$

Hence, the concentration fraction of the open isomer, $M(PMEA)_{op}$, becomes known (Eqs. (20a) and (20b) or (21a) and (21b)).

Regarding the formation degree of the five-membered chelate with the ether O-atom, i.e. $M(PMEA)_{cl/O}$ (Eq. (15)), the same stability is assumed as for $M(PME)_{cl}$ (Section 3), i.e. $K_{I/O}$ for $M(PMEA)_{cl/O}$ equals the corresponding value for $M(PME)_{cl}$ (see Eqs. (1), (9) and Fig. 1). With $K_{I/O}$ and $K_{I/tot}$ known one may now calculate $K_{I/N7}$ (Eq. (16)) from Eq. (20c) or $K_{I/O/N3}$ (Eq. (18)) from Eq. (21c) and hence, the formation degree of the $M(PMEA)_{cl/N7}$ or $M(PMEA)_{cl/O/N3}$ species. Of course, the difference between 100 and the sum of the percentages calculated for $M(PMEA)_{op}$

and $M(PMEA)_{cl/O}$ will also result in % $M(PMEA)_{cl/N7}$ or % $M(PMEA)_{cl/O/N3}$ and hence in $K_{I/N7}$ (Eq. (16)) or $K_{I/O/N3}$ (Eq. (18)). The results of these calculations are presented in Section 6.

5. Comparison of the increased complex stabilities of the M(PME) and M(PMEA) complexes and formation degree of the $M(PME)_{cl}$ and $M(PMEA)_{cl/O}$ isomers

As indicated before (Sections 3 and 4), any kind of metal ion interaction that goes beyond a pure phosphonate coordination in the M(PME) and M(PMEA) complexes must be reflected in an increased complex stability. This is demonstrated in Fig. 2. In this figure plots of log $K^{M}_{M(R\text{-}PO_3)}$ versus $pK^{H}_{H(R\text{-}PO_3)}$ are shown for the 1:1 complexes of Mg^{2+}, Mn^{2+}, and Cu^{2+} with eight simple ligands (see legend of Fig. 2) allowing only an R–PO_3^{2-}–metal ion binding. The corresponding least-squares reference lines, the parameters of which are given in Section 3 in Table 1, define the relation between phosphonate-complex stability and phosphonate-group basicity.

The three solid points in Fig. 2 which refer to Mg(PMEA), Mn(PMEA), and Cu(PMEA) are considerably above their reference lines, thus proving an increased stability for these complexes. However, the analogous observation is also made (crossed points) for the corresponding M(PME) complexes. This clearly proves that equilibrium (1) is operating. Indeed, the significant stability increase for the Mg^{2+} and Mn^{2+} complexes of both ligands is in accordance with the binding of the ether O-atom and contrasts with the observations made for M(5′-AMP) complexes [20,22]; in this latter case macrochelate formation, i.e. N-7 backbinding of a phosphate-coordinated metal ion, occurs only with those metal ions, such as Co^{2+}, Cu^{2+}, Zn^{2+}, or Cd^{2+}, that possess a significant affinity toward N-donor sites.

5.1. *Quantification of the increased complex stabilities*

The vertical distances of the data points due to the M(PME) and M(PMEA) complexes to the reference lines in Fig. 2 evidently correspond to the stability differences defined in Eqs. (12) and (22). In other words, a quantitative evaluation of the situation reflected in Fig. 2 is possible, as already indicated in Section 3, by calculating with the values of $pK^{H}_{H(PME)}$ or $pK^{H}_{H(PMEA)}$ and the straight-line equations summarized in Table 1 the expected (calc) stabilities for $M(PME)_{op}$ or $M(PMEA)_{op}$ complexes having solely a phosphonate–metal ion coordination. The corresponding results are listed in column 3 of Table 2; comparison of them according to Eqs. (12) and (22) with the measured (exper) stability constants, which are given in column 2 of Table 2, leads to the stability differences shown in column 4.

Evidently all the M(PME) and M(PMEA) complexes are more stable than expected on the basis of the basicity of the phosphonate group in the corresponding two ligands; a conclusion already borne out from the data points shown in Fig. 2 for the M(PME) and M(PMEA) complexes with Mg^{2+}, Mn^{2+}, and Cu^{2+}. However, a careful comparison of the data points for the Cu^{2+} complexes in Fig. 2 indicates in addition a higher stability of the Cu(PMEA) complex compared with that of the

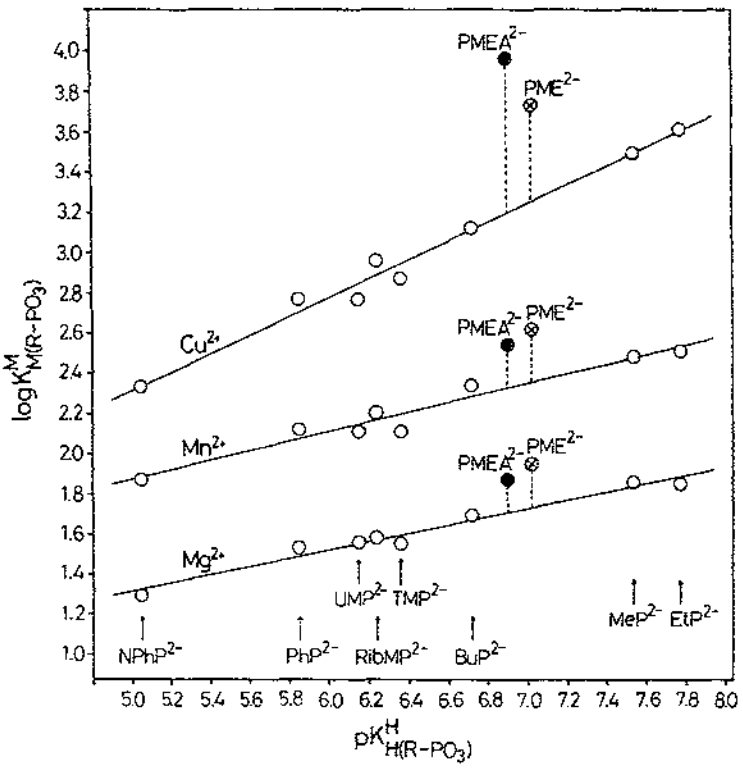

Fig. 2. Evidence for an enhanced stability of several M(PMEA) (●), and M(PME) (⊗) complexes, based on the relationship between log $K^{M}_{M(R\text{-}PO_3)}$ and $pK^{H}_{H(R\text{-}PO_3)}$ for the 1:1 complexes of Mg^{2+}, Mn^{2+}, and Cu^{2+} with some simple phosphate monoester or phosphonate ligands ($R\text{–}PO_3^{2-}$): 4-nitrophenyl phosphate ($NPhP^{2-}$), phenyl phosphate (PhP^{2-}), uridine 5′-monophosphate (UMP^{2-}), D-ribose 5-monophosphate ($RibMP^{2-}$), thymidine 5′-monophosphate (TMP^{2-}), *n*-butyl phosphate (BuP^{2-}), methanephosphonate (MeP^{2-}), and ethanephosphonate (EtP^{2-}) (from left to right) (○). The least-squares lines are drawn through the corresponding eight data sets [7,23]; the equations for these base lines are given in Table 1. The vertical broken lines emphasize the stability differences of the M(PMEA) (●) and M(PME) (⊗) complexes to the corresponding reference lines; these differences equal log $\Delta_{M(PME)}$ (Eq. (12)) and log $\Delta_{M(PMEA)}$ (Eq. (22)).The points due to the equilibrium constants for the PMEA (●) and PME (⊗) systems are taken from Tables 1, 2, and 8 of Ref. [7]. All plotted equilibrium constant values refer to aqueous solutions at 25 °C and $I=0.1$ M ($NaNO_3$).

Cu(PME) species; this observation is confirmed by the corresponding log $\Delta_{M(R\text{-}PO_3)}$ values given in Table 2. Hence, one has to conclude that in Cu(PMEA) the adenine residue is also involved in complex formation (see Section 6).

5.2. *Formation degree of the chelated isomers involving the ether O-atom*

Since the values for log $\Delta_{M(R\text{-}PO_3)}$ are defined analogously for the M(PME) and M(PMEA) complexes (see Eqs. (12) and (22)), their observed increased stabilities

Table 2
Comparison of the measured stabilities, $K^{M}_{M(PME)}$ or $K^{M}_{M(PMEA)}$, of the M(PME) or M(PMEA) complexes with the calculated stabilities, $K^{M}_{M(PME)_{op}}$ or $K^{M}_{M(PMEA)_{op}}$, for the isomers with a sole phosphonate–M^{2+} coordination, as well as a comparison between the stability increases $\log\Delta_{M(PMEA)}$ and $\log\Delta_{M(PME)}$ at 25 °C and $I = 0.1$ M ($NaNO_3$)

M^{2+}	$\log K^{M}_{M(PME)}$ (Eqs. (5,7))[a,b]	$\log K^{M}_{M(PME)_{op}}$ (Eq. (10))[c]	$\log\Delta_{M(PME)}$ (Eq. (12))	
Mg^{2+}	1.95 ± 0.01	1.73 ± 0.03	0.22 ± 0.03	
Ca^{2+}	1.70 ± 0.01	1.56 ± 0.05	0.14 ± 0.05	
Sr^{2+}	1.38 ± 0.03	1.31 ± 0.04	0.07 ± 0.05	
Ba^{2+}	1.33 ± 0.03	1.23 ± 0.04	0.10 ± 0.05	
Mn^{2+}	2.62 ± 0.02	2.35 ± 0.05	0.27 ± 0.05	
Co^{2+}	2.41 ± 0.02	2.12 ± 0.06	0.29 ± 0.06	
Ni^{2+}	2.33 ± 0.02	2.14 ± 0.05	0.19 ± 0.05	
Cu^{2+}	3.73 ± 0.03	3.25 ± 0.06	0.48 ± 0.07	
Zn^{2+}	2.74 ± 0.02	2.40 ± 0.06	0.34 ± 0.06	
Cd^{2+}	3.01 ± 0.02	2.71 ± 0.05	0.30 ± 0.05	
M^{2+}	$\log K^{M}_{M(PMEA)}$ (Eqs. (17,19))[a,d]	$\log K^{M}_{M(PMEA)_{op}}$ (Eq. (14))[c]	$\log\Delta_{M(PMEA)}$ (Eq. (22))	$\Delta\log\Delta$ (Eq. (23))
Mg^{2+}	1.87 ± 0.04	1.71 ± 0.03	0.16 ± 0.05	−0.06 ± 0.06
Ca^{2+}	1.65 ± 0.05	1.54 ± 0.05	0.11 ± 0.07	−0.03 ± 0.09
Sr^{2+}	1.37 ± 0.03	1.30 ± 0.04	0.07 ± 0.05	0.00 ± 0.07
Ba^{2+}	1.30 ± 0.05	1.22 ± 0.04	0.08 ± 0.06	−0.02 ± 0.08
Mn^{2+}	2.54 ± 0.06	2.33 ± 0.05	0.21 ± 0.08	−0.06 ± 0.09
Co^{2+}	2.37 ± 0.03	2.09 ± 0.06	0.28 ± 0.07	−0.01 ± 0.09
Ni^{2+}	2.41 ± 0.05	2.11 ± 0.05	0.30 ± 0.07	0.11 ± 0.09
Cu^{2+}	3.96 ± 0.04	3.19 ± 0.06	0.77 ± 0.07	0.29 ± 0.10
Zn^{2+}	2.66 ± 0.13[e]	2.36 ± 0.06	0.30 ± 0.10[e]	−0.04 ± 0.12
Cd^{2+}	3.00 ± 0.04	2.67 ± 0.05	0.33 ± 0.06	0.03 ± 0.08

[a] The stability constants were measured in aqueous solution via potentiometric pH titrations [7]. All the errors given are 3-times the standard error of the mean value or the sum of the probable systematic errors, whichever is larger. The error limits of all derived data, e.g. logΔ, were calculated according to the error propagation after Gauss.
[b] Acidity constant (see Eq. (11)): $pK^{H}_{H(PME)} = 7.02 \pm 0.01$ [7].
[c] Calculated with $pK^{H}_{H(PME)} = 7.02$ or $pK^{H}_{H(PMEA)} = 6.90$ and the reference-line equations of Table 1; the error limits correspond to the SD values (3σ) in Table 1.
[d] Acidity constants: $pK^{H}_{H_2(PMEA)} = 4.16 \pm 0.02$ (deprotonation of the H^+(N-1) site); $pK^{H}_{H(PMEA)} = 6.90 \pm 0.01$ (deprotonation of the $-P(O)_2(OH)^-$ residue) [7].
[e] No stability constant could be determined owing to precipitation [7]. The above value is an estimate (for details see Ref. [7]).

may be directly compared according to Eq. (23):

$$\Delta \log \Delta = \log \Delta_{M(PMEA)} - \log \Delta_{M(PME)} \quad (23)$$

The corresponding results are listed in the fifth column of the lower part in Table 2:

It is apparent that the values for $\Delta \log \Delta$ are zero within the error limits for clearly eight out of the ten cases.

This means that for the metal ions Mg^{2+}, Ca^{2+}, Sr^{2+}, Ba^{2+}, Mn^{2+}, Co^{2+}, Zn^{2+} (see footnote e of Table 2), and Cd^{2+} the measured increased stability of their M(PMEA) complexes can solely be explained by the formation of the five-membered chelate shown in equilibrium (1), and consequently the adenine residue has no remarkable influence. This result allows Eqs. (9) and (13) (see Section 3) can be applied not only to M(PME) complexes but also to the mentioned eight M(PMEA) systems and that their equilibrium (1) position can be evaluated quantitatively. These results are summarized for both ligand systems in Table 3.

The calculations for K_1 and % $M(PMEA)_{cl/O}$ given in Table 3 confirm that the formation degrees for $M(PMEA)_{cl/O}$ (column 7) and $M(PME)_{cl}$ (column 4) are identical within the error limits for the above-mentioned eight metal ion systems and that consequently these chelates possess the same structure. To conclude, there is no indication of a metal ion–adenine moiety interaction in the M(PMEA) complexes of Mg^{2+}, Ca^{2+}, Sr^{2+}, Ba^{2+}, Mn^{2+}, Co^{2+}, Zn^{2+}, and Cd^{2+}.

6. Formation degree of M(PMEA) isomers involving the adenine residue

The Cu(PMEA) complex is the only clear exception with a *positive* deviation of the value for $\Delta \log \Delta$ (Eq. (23)) in Table 2. Its $\log \Delta_{Cu(PMEA)}$ value is larger by ca. 0.3

Table 3
Extent of chelate formation according to the intramolecular equilibrium (1) in M(PME) and M(PMEA) complexes as quantified by the dimensionless equilibrium constants K_1 (Eqs. (4 and 9)) and $K_{1/O}$ (Eq. (15)), respectively, and the percentages of the $M(PME)_{cl}$ or $M(PMEA)_{cl/O}$ isomers (Eq. (13)) in aqueous solution at 25 °C and $I = 0.1$ M ($NaNO_3$)

M^{2+}	M(PME)			M(PMEA)		
	$\log\Delta_{M(PME)}$ (Eq. (12))[a]	K_1 (Eqs. (4,9))	% $M(PME)_{cl}$ (Eq. (13))	$\log\Delta_{M(PMEA)}$ (Eq. (22))[a]	$K_{1/O}$ (Eqs. (15,9))	% $M(PMEA)_{cl/O}$ (Eq. (13))
Mg^{2+}	0.22±0.03	0.66±0.12	40±4	0.16±0.05	0.45±0.17	31±8
Ca^{2+}	0.14±0.05	0.38±0.16	28±9	0.11±0.07	0.29±0.21	22±13
Sr^{2+}	0.07±0.05	0.17±0.14	15±10	0.07±0.05	0.17±0.14	15±10
Ba^{2+}	0.10±0.05	0.26±0.14	21±9	0.08±0.06	0.20±0.18	17±12
Mn^{2+}	0.27±0.05	0.86±0.23	46±7	0.21±0.08	0.62±0.29	38±11
Co^{2+}	0.29±0.06	0.95±0.28	49±7	0.28±0.07	0.91±0.29	48±8
Ni^{2+}	0.19±0.05	0.55±0.19	35±8	0.30±0.07	*1.00±0.32*[c]	*50±8*[c]
Cu^{2+}	0.48±0.07	2.02±0.47	67±5	0.77±0.07	*4.89±0.98*[c]	*83±3*[c]
Zn^{2+}	0.34±0.06	1.19±0.32	54±7	0.30±0.10[b]	1.00±0.46	50±12
Cd^{2+}	0.30±0.05	1.00±0.25	50±6	0.33±0.06	1.14±0.32	53±7

[a] Values from column 4 of Table 2; see also footnote a of Table 2.
[b] Estimated value; see footnote e of Table 2 and Ref. [7].
[c] The values for $Ni(PMEA)_{cl/O}$ and $Cu(PMEA)_{cl/O}$ are only apparent results (they actually correspond to $M(PMEA)_{cl/tot}$; Eqs. (20b and 21b)) and are therefore printed in *italics* (see Sections 5 and 6). The actual values for $Ni(PMEA)_{cl/O}$ and $Cu(PMEA)_{cl/O}$ are given in Table 4 in Section 6.

log unit than the one for the Cu(PME) system. This means that the adenine residue in the Cu(PMEA) complex clearly has a stability-enhancing effect which goes beyond that of the ether group discussed in Section 5. Consequently, further analysis is necessary by considering the additional intramolecular equilibria outlined in Section 4. In this analysis Ni(PMEA) is included because in this case also an extra stability increase is observed (see column 5 of Table 2) though it is considerably smaller than that for Cu(PMEA) and just barely beyond the error limits. Further, the Cd(PMEA) system is included in the calculations to provide the interested reader with information on how large the percentage of an extra isomer may become without becoming significantly manifested in the experimental data.

As discussed in Section 2, N-1 of $PMEA^{2-}$ (see Fig. 1) is not accessible for a phosphonate-bound metal ion and N-3 can only be reached if the ether O-atom is simultaneously coordinated, while with N-7 a macrochelate may be formed. The latter two possibilities involving N-3 and N-7 are displayed in the equilibrium schemes (2) and (3). The analyses of the corresponding isomeric equilibria have been treated in Section 4; the calculations based on these evaluations are presented in Table 4. In these analyses it is assumed that the stability of the five-membered chelates in the M(PME) species is representative for that of the M(PMEA) ones.

The dimensionless 'overall' equilibrium constant K_I ($=K_{I/tot}$; Eqs. (20) and (21)) follows directly from the experiments (see Section 5; Table 3) and $K_{I/O}$ (Eq. (15)), which quantifies the formation degree of the five-membered chelate with a metal ion bound to the phosphonate group and the ether O-atom (Eq. (1)), has of course the same value in both equilibrium schemes (2) and (3), as it refers to the same formation pathway of the $M(PMEA)_{cl/O}$ isomer; therefore, columns 3–6 and 8 contain the same results in the upper and lower parts of Table 4. Naturally, the values of $K_{I/N7}$ (Eq. (16)) and $K_{I/O/N3}$ (Eq. (18)) are different (column 7), as they refer to different intramolecular equilibria, yet the formation degrees of the $M(PMEA)_{cl/N7}$ (upper part) and $M(PMEA)_{cl/O/N3}$ isomers (lower part) are again identical (column 9). This may seem surprising at first sight, yet the formation degree of the third isomer follows in both cases (Eqs. (2) and (3)) from the difference 100 minus the sum of the percentages for $M(PMEA)_{op}$ and $M(PMEA)_{cl/O}$. This means that the formation degree of the third isomer with the adenine interaction is identical in both cases, be it $M(PMEA)_{cl/N7}$ or $M(PMEA)_{cl/O/N3}$; it reaches approx. 50% in the Cu(PMEA) system (rows 2 and 5 in Table 4), approx. 20% in the Ni(PMEA) system (rows 1 and 4) and for the Cd(PMEA) (rows 3 and 6) and all the other systems (cf. Table 2) it is zero within the error limits, which means it may occur in traces (not exceeding approx. 20%).

At this point the question arises: which of the adenine-bound isomers, $M(PMEA)_{cl/N7}$ or $M(PMEA)_{cl/O/N3}$, is actually formed? Or, are even both isomers present at the same time? With the information currently available these questions cannot be unequivocally answered. However, careful considerations have led to the suggestion [7] that the equilibrium scheme (3) involving the $M(PMEA)_{cl/O/N3}$ isomer is the pertinent one. Indeed, this agrees with the preliminary results obtained from line-broadening ^{1}H-NMR experiments in the presence of paramagnetic Cu^{2+} [25].

Table 4

Intramolecular equilibrium constants for the formation of the various possible isomeric M(PMEA) complexes as defined in the equilibrium schemes (2) and (3), together with the percentages in which the possible isomers occur in aqueous solution at 25 °C and $I = 0.1$ M ($NaNO_3$)[a]

Equilibrium scheme (2) involving N-7 of the adenine residue:								
No.	M^{2+}	$K_1 = K_{1/tot}$ (Eq. (20a))	$\%M(PMEA)_{cl/tot}$ (Eq. (20b))	$\%M(PMEA)_{op}$ (Eq. (20b))	$K_{1/O}$ (Eq. (15))	$K_{1/N7}$ (Eqs. (16,20c))	$\%M(PMEA)_{cl/O}$ (Eqs. (1,2))[b]	$\%M(PMEA)_{cl/N7}$ (Eq. (2))[c]
1	Ni^{2+}	1.00±0.32	50±8	50±8	0.55±0.19	0.45±0.37	28±10	22±13 (19)
2	Cu^{2+}	4.89±0.98	83±3	17±3	2.02±0.47	2.87±1.09	34±10	49±10 (20)
3[d]	Cd^{2+}	1.14±0.32	53±7	47±7	1.00±0.25	0.14±0.41	47±14	6±16 (19)
Equilibrium scheme (3) involving N-3:								
No.	M^{2+}	$K_1 = K_{1/tot}$ (Eq. (21a))	$\%M(PMEA)_{cl/tot}$ (Eq. (21b))	$\%M(PMEA)_{op}$ (Eq. (21b))	$K_{1/O}$ (Eq. (15))	$K_{1/O/N3}$ (Eqs. (18,21c))	$\%M(PMEA)_{cl/O}$ (Eqs. (1,3))[b]	$\%M(PMEA)_{cl/O/N3}$ (Eq. (3))[c]
4	Ni^{2+}	1.00±0.32	50±8	50±8	0.55±0.19	0.82±0.86	28±10	22±13 (25)
5	Cu^{2+}	4.89±0.98	83±3	17±3	2.02±0.47	1.42±0.74	34±10	49±10 (29)
6[d]	Cd^{2+}	1.14±0.32	53±7	47±7	1.00±0.25	0.14±0.43	47±14	6±16 (20)

[a] The values listed in columns 3 and 4 are from columns 6 and 7 in Table 3, respectively. The values given in the fifth column for $\%M(PMEA)_{op}$ follow from $100 - \%M(PMEA)_{cl/tot}$. The constants $K_{1/O}$ of column 6 are from column 3 of Table 3 (see text in Sections 4–6); with the now known values for K_1 and $K_{1/O}$ and Eqs. 20c and 21c those for $K_{1/N7}$ and $K_{1/O/N3}$ may be calculated, respectively (column 7). All error limits in this table correspond to 3-times the standard deviation (3 σ); they were calculated according to the error propagation after Gauss.

[b] These results were calculated via Eq. (15) with $K_{1/O}$ and $\%M(PMEA)_{op}$.

[c] The values for $\%M(PMEA)_{cl/N7}$ or $\%M(PMEA)_{cl/O/N3}$ follow from the difference $\%M(PMEA)_{cl/tot} - \%M(PMEA)_{cl/O}$; $\%M(PMEA)_{cl/N7}$ may also be calculated via Eq. (16) with $K_{1/N7}$ and $\%M(PMEA)_{op}$; analogously $\%M(PMEA)_{cl/O/N3}$ follows from Eq. (18) with $K_{1/O/N3}$ and $\%M(PMEA)_{cl/O}$. The results are the same for both calculation methods (aside from possibly small differences in the last digit due to differences in rounding) yet the error limits (which are given in parenthesis) are understandably larger for the second method.

[d] The Cd(PMEA) system was included only for reasons of comparison; see text in Section 6.

Further information will hopefully also be obtained by including 3-deaza-PMEA^{2-} and 7-deaza-PMEA^{2-} in the studies [25].

The above suggestion about the involvement of N-3 may appear surprising because N-7 of the adenine residue is a very well known binding site for metal ions [13,16–18,20–22,26,27], in contrast to N-3. However, the interaction of metal ions with N-3 of a purine residue has become more and more apparent in the past few years: There are X-ray crystal-structure studies of Pt^{2+} [28a] and Cu^{2+} [28b] complexes of guanine derivatives, of Rh^{+} complexes of 8-azaadenine derivatives [29], as well as of Ni^{2+} complexes formed with neutral adenine [30]. Solution studies with adenosine 2′-monophosphate (2′-AMP^{2-}) show [31] that at least Cu^{2+}, and possibly also Ni^{2+} and Cd^{2+}, forms macrochelates involving N-3. Indeed, the formation degree of Cu(2′-AMP)$_{cl/N3}$ is comparable with that of Cu(PMEA)$_{cl/O/N3}$; moreover, the corresponding M(2′-AMP)$_{cl/N3}$ chelates with Ni^{2+} and Cd^{2+} also form only in relatively low concentrations [31] just like those with PMEA^{2-} (cf. Table 4).

7. Solvent-dependent metal ion–adenine recognition. The effect of mixed solvents on the formation degree of the Cu(PMEA) isomers

7.1. Justification for studies of this kind

To what extent is the formation degree of the various M(PMEA) isomers affected by the polarity of the solvent? Does a reduced solvent polarity favor or inhibit chelate formation? Answers to questions of this kind are of general interest because our knowledge in this respect is extremely scarce even though it is now well established that the so-called 'effective' or 'equivalent solution' dielectric constants in proteins [32] or active-site cavities of enzymes [33] are reduced compared to that in bulk water; i.e., the activity of water is decreased [34] due to the presence of aliphatic and aromatic amino acid side chains at the protein–water interface.

For example, for the active-site cavities of bovine carbonic anhydrase and carboxy peptidase A the 'effective' dielectric constants are estimated to be 35 and <70, respectively [33]. By employing aqueous solutions that contain 1,4-dioxane one may expect to simulate to some degree the situation in such cavities; e.g., water containing 30 or 50% (v/v) 1,4-dioxane exhibits dielectric constants of about 53 and 35, respectively [35].

7.2. The effect of the solvent on the size of the equilibrium constants

In the preceding Section 6 we have seen that in aqueous solution all three Cu(PMEA) isomers (Eqs. (2) and (3)) occur with a significant formation degree (cf. Table 4). Therefore, the Cu(PMEA) system was also studied [9] in 30% and 50% (v/v) dioxane–water mixtures to address the questions raised in Section 7.1. Of course, for a quantitative evaluation it was necessary to include in the study the Cu(PME) system. The corresponding results are summarized in Table 5.

In addition to the equilibrium data given in Table 5, reference lines for $\log K^{Cu}_{Cu(R\text{-}PO_3)}$ versus $pK^{H}_{H(R\text{-}PO_3)}$ plots had to be established [9,36]. These reference line plots are shown in Fig. 3, where the corresponding data pairs for the Cu^{2+}/PME^{2-} and Cu^{2+}/PMEA^{2-} systems are also inserted. The resulting six solid

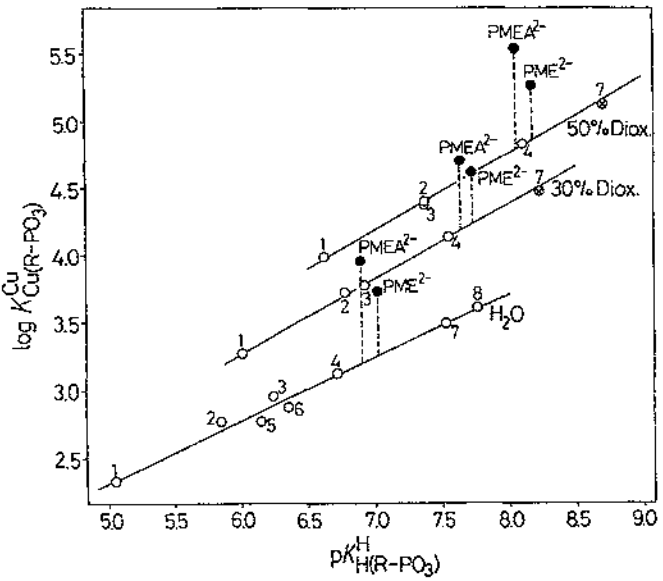

Fig. 3. Evidence for an enhanced stability of the Cu(PME) and Cu(PMEA) (●) complexes in 1,4-dioxane–water mixtures as solvents based on the relationship between log $K^{Cu}_{Cu(R\text{-}PO_3)}$ and $pK^{H}_{H(R\text{-}PO_3)}$ for the Cu^{2+} 1:1 complexes of 4-nitrophenyl phosphate (1), phenyl phosphate (2), D-ribose 5-monophosphate (3), *n*-butyl phosphate (4), uridine 5′-monophosphate (5), thymidine 5′-monophosphate (6), methanephosphonate (7), and ethanephosphonate (8) in water and in water containing 30 or 50% (v/v) 1,4-dioxane. The least-squares lines are drawn in each case through the data sets shown (○) [7,36]; the equations for these reference lines are given in Ref. [9]. The data points due to the methanephosphonate system in the mixed solvents (⊗) (see Ref. [9]) are shown to prove that simple phosphonates fit within the experimental error limits on the reference lines established with phosphate monoester systems (see also Ref. [9]). The points due to the Cu^{2+} 1:1 complexes formed with PME^{2-} and $PMEA^{2-}$ (●) in the three mentioned solvents are inserted for comparison (see Table 5 and Section 7). The vertical broken lines emphasize the stability differences to the corresponding reference lines; these differences equal log $\Delta_{Cu(R\text{-}PO_3)}$ (see Eqs. (12) and (22)). All the plotted equilibrium constants refer to 25 °C and $I = 0.1$ M ($NaNO_3$). Reproduced from Ref. [9] by permission of the American Chemical Society.

points are considerably above the reference lines in all three solvents, thus proving increased stabilities. These increased stabilities, i.e., their vertical distance to the reference lines, are quantified via the log $\Delta_{M(PME)}$ and log $\Delta_{M(PMEA)}$ values given in column 9 of Table 5. Further, as also seen in Fig. 3, the values calculated for Δ log Δ (Eq. (23); column 10 of Table 5) confirm that in all three solvents the adenine residue of $PMEA^{2-}$ participates in Cu^{2+} binding.

Of course, for Cu(PME) again only equilibrium (1) is operating; the results of the corresponding mathematical evaluation (see Section 3) are given in the upper part of Table 6. It is remarkable that the formation degree of $Cu(PME)_{el}$ is rather independent of the solvent (column 4) despite the fact that the overall stability constant log $K^{Cu}_{Cu(PME)}$ increases by more than 1.5 log units in changing the solvent from water to a 50% dioxane–water mixture (see column 7 of Table 5).

Regarding Cu(PMEA), values for K_1 ($= K_{1/tot}$) as defined by Eqs. (20) and (21)

Table 5

Negative logarithms of the acidity constants of $H(PME)^-$ (Eq. (11)) and $H_2(PMEA)^{\pm}$ and logarithms of the stability constants, $\log K^{Cu}_{Cu(R\text{-}PO_3)}$, of the Cu(PME) (Eqs. (5 and 7)) and Cu(PMEA) complexes (Eqs. (17a and 19a)) as determined by potentiometric pH titrations in water and in water containing 30 or 50% (v/v) 1,4-dioxane at 25 °C and $I = 0.1$ M ($NaNO_3$).[a] The calculated logarithms of the stability constants for a pure phosphonate–Cu^{2+} coordination, $\log K^{Cu}_{Cu(R\text{-}PO_3)_{op}}$ (Eqs. (10 and 14)), are based on straight-line equations quantifying the relationship between complex stability and phosphonate group basicity[b] and the $pK^{H}_{H(R\text{-}PO_3)}$ values of $H(PME)^-$ and $H(PMEA)^-$. Some properties[c] of the mentioned solvents are also listed as well as various stability differences of the Cu^{2+} complexes considered

$R\text{–}PO_3^{2-}$	% Dioxane (v/v)	mol fraction	ε[c]	$pK^{H}_{H_2(R\text{-}PO_3)}$[d]	$pK^{H}_{H(R\text{-}PO_3)}$[e]	$\log K^{Cu}_{Cu(R\text{-}PO_3)}$	$\log K^{Cu}_{Cu(R\text{-}PO_3)_{op}}$[b]	$\log\Delta_{M(R\text{-}PO_3)}$ (Eqs. (12,22))	$\Delta\log\Delta$ (Eq. (23))
PME^{2-}	0	0	78.5		7.02 ± 0.01	3.73 ± 0.03	3.25 ± 0.06	0.48 ± 0.07	
	30	0.083	52.7		7.73 ± 0.02	4.62 ± 0.03	4.23 ± 0.03	0.39 ± 0.04	
	50	0.175	35.2		8.17 ± 0.03	5.27 ± 0.06	4.86 ± 0.03	0.41 ± 0.07	
$PMEA^{2-}$	0	0	78.5	4.16 ± 0.02	6.90 ± 0.01	3.96 ± 0.04[e]	3.19 ± 0.06	0.77 ± 0.07	0.29 ± 0.10
	30	0.083	52.7	3.79 ± 0.01	7.64 ± 0.01	4.70 ± 0.05[e]	4.18 ± 0.03	0.52 ± 0.06	0.13 ± 0.07
	50	0.175	35.2	3.73 ± 0.01	8.05 ± 0.01	5.54 ± 0.07[e]	4.79 ± 0.03	0.75 ± 0.08	0.34 ± 0.11

[a] See footnote a of Table 2. The above data are from Ref. [9].

[b] The parameters of the straight-line equations used for the above calculations are given in entries 1b, 2 and 3 of Table 2 in Ref. [9].

[c] The dielectric constants (ε) for the dioxane–water mixtures are interpolated from the data given in Ref. [35].

[d] These acidity constants refer to the deprotonation of the H^+(N-1) site of the adenine residue in $H_2(PMEA)^{\pm}$.

[e] These acidity constants are due to the deprotonation of the $-P(O)_2(OH)^-$ group in H(PME) or H(PMEA).

Table 6
Extent of chelate formation according to equilibrium (1) in the Cu(PME) species as quantified by the dimensionless equilibrium constant K_I (Eq. (4)) and the percentage of $Cu(PME)_{cl}$ (Eq. (13)) in aqueous solution and in water containing 30 or 50% (v/v) 1,4-dioxane at 25 °C and $I=0.1$ M ($NaNO_3$).[a] In addition the overall values $K_{I/tot}$ ($=K_I$; Eqs. (20a and 21a)) and % $Cu(PMEA)_{cl/tot}$ for the Cu(PMEA) systems in the mentioned solvents are given

%Dioxane (v/v)	Cu(PME)		
	$\log\Delta_{Cu(PME)}$ (Eq. (12))[a]	K_I (Eqs. (4,9))	$\%Cu(PME)_{cl}$ (Eq. (13))
0	0.48±0.07	2.02±0.47	67±5
30	0.39±0.04	1.45±0.24	59±4
50	0.41±0.07	1.57±0.40	61±6
%Dioxane (v/v)	Cu(PMEA)		
	$\log\Delta_{Cu(PMEA)}$ (Eq. (22))[a]	$K_I=K_{I/tot}$ (Eqs. (20a,21a))[b]	$\%Cu(PMEA)_{cl/tot}$ (Eqs. (20b,21b))[b]
0	0.77±0.07	4.89±0.98	83±3
30	0.52±0.06	2.31±0.44	70±4
50	0.75±0.08	4.62±0.99	82±3

[a] The values for $\log\Delta_{Cu(PME)}$ and $\log\Delta_{Cu(PMEA)}$ and their error limits (3σ) are from column 9 of Table 5 [9]; see also footnote a of Table 2.
[b] Regarding these values see also Table 7 and the text in Section 7.

can be calculated with the stability differences $\log\Delta_{Cu(PMEA)}$ (Eq. (22)); these data together with those for $Cu(PMEA)_{cl/tot}$ (Eqs. (20b) and (21b)), which are needed for the analysis of the three-isomer situation, are given in the lower part of Table 6. Application of the procedure described in Section 4 and already used in Section 6 leads to the results for the equilibrium schemes (2) and (3) as summarized in Table 7. The considerations given in Section 6 in connection with the analogous Table 4 also apply here for Table 7 and are therefore not repeated.

7.3. Dependence of the extent of the metal ion–adenine interaction on the solvent composition

Though there are indications (see Section 6) that N-3 is the pertinent binding site for Cu^{2+} and that consequently (mainly) equilibrium scheme (3) is operating, a final decision between the results given in the upper (Eq. (2)) and lower parts (Eq. (3)) of Table 7 cannot yet be made. Therefore, the isomers with the Cu^{2+}–adenine interaction, which definitely exists be it via N-3 or N-7, are now designated simply $Cu(PMEA)_{cl/Ad}$. It is most interesting to note from the results in Table 7 (see rows 2 and 5) that the addition of 1,4-dioxane to an aqueous solution containing Cu(PMEA) initially lowers the formation degree of the $Cu(PMEA)_{cl/Ad}$ isomer, yet upon the addition of more 1,4-dioxane it increases again.

Table 7
Intramolecular equilibrium constants according to the equilibrium schemes (2) and (3) for the formation of the various possible isomeric Cu(PMEA) complexes, together with the percentages in which the possible isomers occur in aqueous solution and in water containing 30 or 50% (v/v) 1,4-dioxane at 25 °C and $I = 0.1$ M ($NaNO_3$)[a]

Equilibrium scheme (2) involving N-7 of the adenine residue:								
No.	%Dioxane (v/v)	$K_I = K_{I/tot}$ (Eq. (20a))	$\%Cu(PMEA)_{cl/tot}$ (Eq. (20b))	$\%Cu(PMEA)_{op}$ (Eq. (20b))	$K_{I/O}$ (Eqs. (15))	$K_{I/N7}$ (Eqs. (16,20c))	$\%Cu(PMEA)_{cl/O}$ (Eqs. (1,2))[b]	$\%\{Cu(PMEA)_{cl/N7}$ (Eq. (2))[c]
1	0	4.89±0.98	83±3	17±3	2.02±0.47	2.87±1.09	34±10	49±10 (20)
2	30	2.31±0.44	70±4	30±4	1.45±0.23	0.86±0.51	44±9	26±10 (16)
3	50	4.62±0.99	82±3	18±3	1.57±0.40	3.05±1.06	28±9	54±9 (21)
Equilibrium scheme (3) involving N-3:								
No.	%Dioxane (v/v)	$K_I = K_{I/tot}$ (Eq. (21a))	$\%Cu(PMEA)_{cl/tot}$ (Eq. (21b))	$\%Cu(PMEA)_{op}$ (Eq. (21b))	$K_{I/O}$ (Eq. (15))	$K_{I/O/N3}$ (Eqs. (18,21c))	$\%Cu(PMEA)_{cl/O}$ (Eqs. (1,3))[b]	$\%Cu(PMEA)_{cl/O/N3}$ (Eq. (3))[c]
4	0	4.89±0.98	83±3	17±3	2.02±0.47	1.42±0.74	34±10	49±10 (29)
5	30	2.31±0.44	70±4	30±4	1.45±0.23	0.59±0.40	44±9	26±10 (19)
6	50	4.62±0.99	82±3	18±3	1.57±0.40	1.94±0.97	28±9	54±9 (32)

[a] The values in columns 3 and 4 are from the corresponding columns in Table 6. Otherwise footnote a of Table 4 applies also here.
[b,c] See the corresponding footnotes in Table 4 as well as the text in Section 7.

A similar observation was made [37] for Cu(5′-AMP), for which an isomeric equilibrium exists between a simple phosphate-bound isomer, $Cu(5'\text{-}AMP)_{op}$, and a macrochelated species involving the phosphate group and the N-7 site, designated $Cu(5'\text{-}AMP)_{cl}$. To illustrate this point further the pertinent results from Ref. 37 are plotted in Fig. 4 together with those of Table 7. The formation degree of both $Cu(5'\text{-}AMP)_{cl}$ and $Cu(PMEA)_{cl/Ad}$ passes through a minimum upon the addition of 1,4-dioxane to aqueous solutions of these complex systems.

This fascinating observation means that independent of the fact that the overall stability constants $\log K^{Cu}_{Cu(5'\text{-}AMP)}$ [37] and $\log K^{Cu}_{Cu(PMEA)}$ (Table 5, column 7) increase continuously upon the addition of dioxane, the formation degree of the various isomers is altered differently and as yet unpredictably. Considering that in active-site cavities of metalloproteins the 'solvent' polarity [32,33] and the activity of water [34] are reduced, this is a remarkable result because it demonstrates how nature may alter the structure of a substrate simply by moving it along a protein surface from a more polar into a more apolar region or vice versa.

8. Formation of mixed ligand complexes also involving purine-stacked isomers

A further aspect that warrants consideration in studies aimed at elucidating the properties of PMEA is its possible tendency to undergo stacking; purine derivatives are well known for this property [38] and accordingly it is also expected for PMEA. With this in mind a study was undertaken [8] of mixed ligand systems consisting

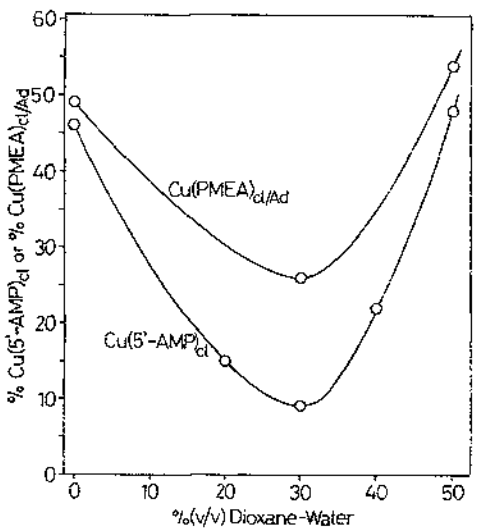

Fig. 4. Formation degree of the adenine-chelated species (equilibrium schemes (2) and (3)) in the binary Cu^{2+} 1:1 complex systems with $PMEA^{2-}$ (see Table 7) and $5'\text{-}AMP^{2-}$ (from Ref. [37]) as a function of the percentage of 1,4-dioxane added to the aqueous reagent mixtures at 25 °C and $I = 0.1$ M ($NaNO_3$). $Cu(PMEA)_{cl/Ad}$ represents $Cu(PMEA)_{cl/O/N3}$ and/or $Cu(PMEA)_{cl/N7}$ (see text in Section 7), while $Cu(5'\text{-}AMP)_{cl}$ represents the macrochelate involving the phosphate group and N-7 of the purine moiety [20,22]. Reproduced from Ref. [9] by permission of the American Chemical Society.

of Cu^{2+}, $PMEA^{2-}$, and a heteroaromatic amine (arm), i.e., 2,2'-bipyridyl (bpy) or 1,10-phenanthroline (phen), with the aim of quantifying the formation degree of the expected intramolecular stacks (cf. Fig. 5) and to compare the results with the situation in the corresponding Cu(arm)(AMP) complexes. For these latter species the position of the intramolecular equilibrium (24) (rib = ribose) has also been determined [39]:

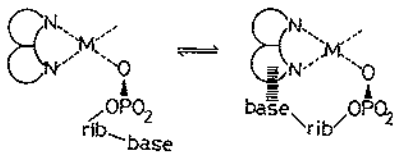

(24)

A major obstacle in such an attempt is the already mentioned metal ion-ether oxygen interaction (Eq. (1)), i.e., the five-membered chelate ring formation in the binary M(PMEA) complexes (Sections 5 and 6) [7], because such an interaction has to a certain extent also to be expected in Cu(arm)(PMEA) complexes and this of course will affect the formation of the intramolecular stacks between the purine moiety of $PMEA^{2-}$ and the aromatic rings of bpy or phen (cf. Fig. 5). To overcome this problem again PME^{2-} (see Fig. 1) was included in the study [8], as this ligand should be able to undergo an ether oxygen–metal ion interaction in mixed ligand complexes to the same extent as $PMEA^{2-}$, yet it cannot form any stacks; hence, the separation of these two different types of intramolecular interactions should become possible.

8.1. *Stabilities of Cu(arm)(R–PO$_3$) complexes*

The results for the PME systems are summarized in the upper part of Table 8. As the straight-line equations for $\log K^{Cu(arm)}_{Cu(arm)(R\text{-}PO_3)}$ versus $pK^{H}_{H(R\text{-}PO_3)}$ plots are known [8] the measured stability constants of the ternary Cu(arm)(PME) complexes can

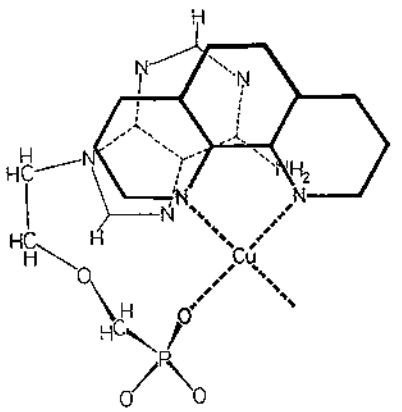

Fig. 5. Tentative and simplified structure of a species with an intramolecular stack for Cu(phen)(PMEA) in solution.

Table 8
Quantification of the stability increase via logΔ (analogous to Eqs. (12) and (22)) for the Cu(arm)(PME) and Cu(arm)(PMEA) complexes, and extent of the intramolecular chelate formation (Eq. (13)) in the Cu(arm)(PME) complexes at 25 °C and $I = 0.1$ M ($NaNO_3$): the results for the corresponding binary Cu(PME) complex are given for comparison

M^{2+}	$\log K^{M}_{M(PME)}$ (Eqs. (5,7))[a]	$\log K^{M}_{M(PME)_{op}}$ (Eq. (10))[b]	$\log\Delta_{PME}$ (Eq. (12))[c]	K_i (Eqs. (4,9))[c]	$\%M(PME)_{cl}$ (Eq. (13))[c,d]
Cu^{2+}	3.73 ± 0.03	3.25 ± 0.06	0.48 ± 0.07	2.02 ± 0.47	67 ± 5
$Cu(bpy)^{2+}$	3.86 ± 0.03	3.27 ± 0.07	0.59 ± 0.08	2.89 ± 0.68	74 ± 5
$Cu(phen)^{2+}$	3.90 ± 0.04	3.28 ± 0.06	0.62 ± 0.07	3.17 ± 0.69	76 ± 4
M^{2+}	$\log K^{M}_{M(PMEA)}$ (Eq. (29a))[a]	$\log K^{M}_{M(PMEA)_{op}}$ (Eq. (26))[b]	$\log\Delta_{PMEA}$ (Eq. (22))[c]	$K_i = K_{i/tot}$ (Eq. (30))[c]	$\%Cu(arm)(PMEA)_{int/tot}$ (cf. Eqs. (30b,30c))
$Cu(bpy)^{2+}$	4.70 ± 0.02	3.22 ± 0.07	1.48 ± 0.07	29.20 ± 4.87	96.69 ± 0.53
$Cu(phen)^{2+}$	4.97 ± 0.03	3.23 ± 0.06	1.74 ± 0.07	53.95 ± 8.86	98.18 ± 0.29

[a] See footnote a of Table 2. The constants are from Ref. [8].
[b] These constants were calculated with the pK_a values 7.02 and 6.90 for $H(PME)^-$ and $H(PMEA)^-$, respectively (see footnotes in Table 2), and the straight-line equations given in Table 5 of Ref. [8]; the corresponding error limits are 3-times the SD values (see Table 5 in Ref. [8]).
[c] The error limits for logΔ, K_i and $\%M(PME)_{cl}$ were calculated according to the error propagation after Gauss; the same applies for the lower part of the table.
[d] See equilibrium (1).

be evaluated in the way described in Section 3; these results are also listed in the upper part of Table 8. Comparison of the data in columns 2–4 proves that the Cu(arm)(PME) species are indeed more stable than expected on the basis of the basicity of the phosphonate group of PME^{2-}. Consequently via Eqs. (9) and (13) the intramolecular equilibrium constant K_I and the percentage for the closed species, $Cu(arm)(PME)_{cl}$, can be calculated. It is evident that the formation degree of the five-membered chelate involving the ether O-atom (Table 8, column 6) is at least as pronounced in the mixed ligand Cu(arm)(PME) complexes as in the parent Cu(PME) complex; in other words, equilibrium (1) is also operating in the ternary Cu(arm)(PME) complexes.

The experimentally measured stability constants of the ternary Cu(arm)(PMEA) complexes as well as the calculated stabilities of the 'open' isomers are listed in columns 2 and 3, respectively, in the lower part of Table 8. The stability differences $\log \Delta_{Cu(arm)(PMEA)}$ (= $\log \Delta_{PMEA}$ in Table 8) derived according to Eq. (22) are given in the fourth column; these values are positive, thus confirming that additional intramolecular interactions occur in these $PMEA^{2-}$ complexes, giving rise to a higher stability than expected on the basis of the basicity of the $PMEA^{2-}$ phosphonate group. However, most important is the fact that the $\log \Delta_{Cu(arm)(PMEA)}$ values are also significantly larger than those for $\log \Delta_{Cu(arm)(PME)}$, as a comparison between the corresponding values in the upper and lower parts of Table 8 (column 4) demonstrates. This additional stability enhancement is more clearly seen in Fig. 6, where plots of $\log K^{Cu(arm)}_{Cu(arm)(R\text{-}PO_3)}$ versus $pK^{H}_{H(R\text{-}PO_3)}$ are shown. The broken line refers to the coordination of $R\text{–}PO_3^{2-}$ to $Cu(bpy)^{2+}$ and the solid line to the corresponding reaction with $Cu(phen)^{2+}$; it should be noted that here $R\text{–}PO_3^{2-}$ represents phosphonates with a group R which is unable to undergo any kind of interaction within the complexes. Clearly, the most remarkable observation is that the points due to Cu(arm)(PME) and Cu(arm)(PMEA) are significantly above the correlation lines; in addition, those for Cu(bpy)(PMEA) and Cu(phen)(PMEA) are even about 1 log unit above the points of the corresponding Cu(arm)(PME) complexes, definitely proving that further interactions must occur in the Cu(arm)(PMEA) species, i.e., that intramolecular stacks of the type shown in Fig. 5 are formed.

The vertical distances in Fig. 6 between the points due to Cu(arm)(PME) and Cu(arm)(PMEA) and the base lines are evidently a measure of the extent of the intramolecular interactions occurring in these complexes and the mentioned distances also correspond here to the log Δ values as defined in Eqs. (12) and (22), respectively. Of course, as already pointed out above, the increased stability of the Cu(arm)(PME) species is due to the formation of the five-membered chelates shown in equilibrium (1) and quantified in the upper part of Table 8. Further, PME^{2-} and $PMEA^{2-}$ (see Fig. 1) are equally well suited for the formation of the mentioned five-membered chelates, but stack formation is possible only with $PMEA^{2-}$. Hence, for the Cu(arm)(PMEA) species the existence of (at least) three different isomers has to be considered in solution.

8.2. Evaluation and mathematical treatment of the Cu(arm)(PMEA) systems

The formation of the five-membered chelates involving the ether oxygen of PME^{2-} or $PMEA^{2-}$ certainly occurs within the equatorial part of the coordination sphere

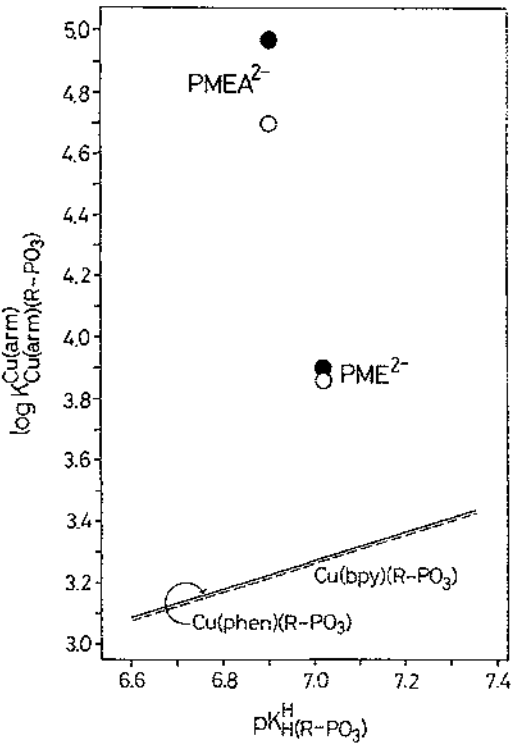

Fig. 6. Evidence for an enhanced stability of the Cu(arm)(PME) and Cu(arm)(PMEA) complexes based on the relationship between log $K^{Cu(arm)}_{Cu(arm)(R\text{-}PO_3)}$ and $pK^{H}_{H(R\text{-}PO_3)}$ for the ternary Cu(bpy)(PME) and Cu(bpy)(PMEA) (○), as well as for the Cu(phen)(PME) and Cu(phen)(PMEA) (●) complexes in aqueous solution at $I=0.1$ M ($NaNO_3$) and 25 °C. The plotted data are from Table 8 in Section 8 [8]. The two reference lines represent the log K versus pK_a relationship for Cu(arm)(R-PO_3) complexes; it should be emphasized that R–PO_3^{2-} symbolizes here phosphonates (or phosphate monoesters) with an R group unable to undergo any kind of hydrophobic, stacking or other type of interaction; the broken line holds for arm = bpy and the solid line for arm = phen. Both straight lines are calculated with the parameters listed in Table 5 of Ref. [8] and they represent the situation for ternary complexes without an intramolecular ligand–ligand interaction. Redrawn in a slightly altered way from Ref. [8] with permission of the Royal Chemical Society.

of Cu^{2+} because only weak interactions are possible with the apical positions [40,41] and the stability increase as expressed by log $\Delta_{Cu(arm)(PME)}$ with about 0.6 is substantial indeed (cf. Table 8). The corresponding chelated isomer with $PMEA^{2-}$ is now designated $Cu(arm)(PMEA)_{cl/O}$. Careful considerations [8] have led to the conclusion that the adenine residue in such a species cannot stack well with the aromatic rings of the also equatorially coordinated arm. A substantial and strain-free overlap is possible only if the ether oxygen is not equatorially coordinated to Cu^{2+}; this situation is depicted in Fig. 5. However, from molecular models it becomes evident that an *apical* ether oxygen coordination and simultaneous stack formation would be compatible with each other. Hence, there are various intramolecularly stacked Cu(arm)(PMEA) species possible, including those with somewhat different orienta-

tions of the aromatic rings toward each other. As there is at present no way to distinguish these various isomers and conformers from each other, all the stacked species (st) are treated together and designated Cu(arm)(PMEA)$_{st}$. The sum of these reasonings then gives rise to the equilibrium scheme (25), where the pure phosphonate coordinated (or 'open') isomer is designated Cu(arm)(PMEA)$_{op}$.

$$\begin{array}{l} \qquad\qquad\qquad\qquad\qquad\qquad\quad \text{Cu(arm)(PMEA)}_{cl/O} \\ \qquad\qquad\qquad\qquad\qquad\qquad\quad \diagup\!\!\diagup\ K_{I/O} \\ \text{Cu(arm)}^{2+} + \text{PMEA}^{2-} \xrightleftharpoons{K^{Cu(arm)}_{Cu(arm)(PMEA)_{op}}} \text{Cu(arm)(PMEA)}_{op} \\ \qquad\qquad\qquad\qquad\qquad\qquad\quad \diagdown\!\!\diagdown\ K_{I/st} \\ \qquad\qquad\qquad\qquad\qquad\qquad\quad \text{Cu(arm)(PMEA)}_{st} \end{array} \tag{25}$$

It is evident that the upper branch of this equilibrium scheme reflects equilibrium (1) while the lower branch is analogous to equilibrium (24).

Maybe one should mention in this context that a Cu(arm)$^{2+}$ isomer analogous to M(PMEA)$_{cl/N7}$ (Eq. (2)) or M(PMEA)$_{cl/O/N3}$ (Eq. (3)) can hardly form owing to steric hindrance or even not at all owing to the absence of further equatorial sites in the coordination sphere of Cu^{2+}, respectively. Of course, an elimination of arm from the coordination sphere of Cu^{2+} via a binding site at the adenine residue is also not possible to any significant extent. Hence, isomers of the indicated kind will not form to any significant degree among the various Cu(arm)(PMEA) species. Evidently, equilibrium scheme (25) thus describes the actual situation well.

Based on equilibrium scheme (25), which is analogous to scheme (2), one may proceed as described in Section 4 and define the following expressions:

$$K^{Cu(arm)}_{Cu(arm)(PMEA)_{op}} = [\text{Cu(arm)(PMEA)}_{op}]/([\text{Cu(arm)}^{2+}][\text{PMEA}^{2-}]) \tag{26}$$

$$K_{I/O} = [\text{Cu(arm)(PMEA)}_{cl/O}]/[\text{Cu(arm)(PMEA)}_{op}] \tag{27}$$

$$K_{I/st} = [\text{Cu(arm)(PMEA)}_{st}]/[\text{Cu(arm)(PMEA)}_{op}] \tag{28}$$

For the experimentally accessible equilibrium constant it holds,

$$K^{Cu(arm)}_{Cu(arm)(PMEA)} = \frac{[\text{Cu(arm)(PMEA)}]}{[\text{Cu(arm)}^{2+}][\text{PMEA}^{2-}]} \tag{29a}$$

$$= \frac{([\text{Cu(arm)(PMEA)}_{op}] + [\text{Cu(arm)(PMEA)}_{cl/O}] + [\text{Cu(arm)(PMEA)}_{st}])}{[\text{Cu(arm)}^{2+}][\text{PMEA}^{2-}]} \tag{29b}$$

$$= K^{Cu(arm)}_{Cu(arm)(PMEA)_{op}} + K_{I/O} \cdot K^{Cu(arm)}_{Cu(arm)(PMEA)_{op}} + K_{I/st} \cdot K^{Cu(arm)}_{Cu(arm)(PMEA)_{op}} \tag{29c}$$

$$= K^{Cu(arm)}_{Cu(arm)(PMEA)_{op}} (1 + K_{I/O} + K_{I/st}) \tag{29d}$$

and for the intramolecular interactions one obtains,

$$K_I = K_{I/tot} = \frac{K^{Cu(arm)}_{Cu(arm)(PMEA)}}{K^{Cu(arm)}_{Cu(arm)(PMEA)_{op}}} - 1 = 10^{\log \Delta} - 1 \tag{30a}$$

$$= \frac{[Cu(arm)(PMEA)_{int/tot}]}{[Cu(arm)(PMEA)_{op}]} \tag{30b}$$

$$= \frac{([Cu(arm)(PMEA)_{cl/O}] + [Cu(arm)(PMEA)_{st}])}{[Cu(arm)(PMEA)_{op}]} \tag{30c}$$

$$= K_{I/O} + K_{I/st} \tag{30d}$$

where $Cu(arm)(PMEA)_{int/tot}$ refers to the sum of all the species present with such an interaction. Clearly, in those cases where the stacked species, i.e., $Cu(arm)(PMEA)_{st}$, are not formed, the above equations reduce to the two-isomer problem (equilibrium (1)) treated in Eqs. (6)–(13) in Section 3.

8.3. *Formation degree of the various species formed in the Cu(arm)(PMEA) systems*

It is evident that K_I ($= K_{I/tot}$; Eq. (30)) can be calculated according to Eq. (30a) because the values for $\log \Delta_{Cu(arm)(PMEA)}$ (Eq. (22)) are known and listed in the lower part of Table 8 ($= \log \Delta_{PMEA}$). These K_I values together with the formation degree of $Cu(arm)(PMEA)_{int/tot}$ (see Eqs. (30b, 30c)) are also given in the lower part of Table 8, i.e., in columns 5 and 6, respectively. From this information follows also the formation degree of the open isomers, $Cu(arm)(PMEA)_{op}$ (see column 4 of Table 9). For the calculation of the formation degree of the species forming the five-membered chelate with the ether oxygen, i.e., $Cu(arm)(PMEA)_{cl/O}$ (Eq. (27)) again (cf. Sections 4, 5.2 and 6) the justified assumption is made that the species $Cu(arm)(PME)_{cl}$ (Table 8) and $Cu(arm)(PMEA)_{cl/O}$ have the same stability. Knowing now K_I and $K_{I/O}$ one can calculate $K_{I/st}$ from Eq. (30d) and, hence, the formation degree of the $Cu(arm)(PMEA)_{st}$ species. The results of these calculations are listed in Table 9.

Considering equilibrium scheme (25) and the corresponding data summarized in Table 9, various aspects are immediately evident. (i) All three structurally different species of Cu(arm)(PMEA) are formed in noticeable amounts. (ii) The stacked species (Fig. 5) are clearly the dominating ones, reaching a formation degree of about 90%. (iii) Consequently, the formation degree of the five-membered chelates involving the ether O-atom is suppressed to about 10% (and below) compared to the approx. 75% present in the Cu(arm)(PME) systems (see Table 8).

A further aspect that deserves emphasizing is the fact that the values for $K_{I/st}$ of Cu(bpy)(PMEA) and Cu(phen)(PMEA) differ by a factor of about 2, i.e., 26.31 ($\pm$4.92) versus 50.78 ($\pm$8.89) (Table 9). This is the result of the smaller aromatic ring system of 2,2′-bipyridyl compared to that of 1,10-phenanthroline. Indeed, the same factor of about 2 was also observed for Cu(bpy)(5′-AMP) and Cu(phen)(5′-AMP) with the K_I values for stack formation of 4.37 ($\pm$1.02) versus 8.77 ($\pm$1.81) [39]. Hence, it appears that this is a general phenomenon for the

Table 9
Intramolecular equilibrium constants for the formation of the three differently structured Cu(arm)(PMEA) species shown in the equilibrium scheme (25), together with the percentages in which these species occur in aqueous solution at 25 °C and $I = 0.1$ M ($NaNO_3$)[a]

arm	$K_I = K_{I/tot}$ (Eq. (30a))	%Cu(arm)(PMEA)$_{int/tot}$ (cf. Eqs. (30b,30c))	%Cu(arm)(PMEA)$_{op}$ (Eq. (25))	$K_{I/O}$ (Eq. (27))	$K_{I/st}$ (Eq. (28,30d))	%Cu(arm)(PMEA)$_{cl/O}$ (Eqs. (1,25))[b]	%Cu(arm)(PMEA)$_{st}$ (Eq. (25))[c]
bpy	29.20 ± 4.87	96.69 ± 0.53	3.31 ± 0.53	2.89 ± 0.68	26.31 ± 4.92	10 ± 3	87 ± 3 (21)
phen	53.95 ± 8.86	98.18 ± 0.29	1.82 ± 0.29	3.17 ± 0.69	50.78 ± 8.89	6 ± 2	92 ± 2 (25)

[a] The values listed in the second column are from the fifth column in the lower part of Table 8. These values for $K_I = K_{I/tot}$ follow from Eq. (30a) and %Cu(arm)(PMEA)$_{int/tot}$ is calculated analogously to Eq. (13). The values given in the fourth column for %Cu(arm)(PMEA)$_{op}$ follow from 100 − %Cu(arm)(PMEA)$_{int/tot}$. The constants $K_{I/O}$ of column 5 are from the upper part in column 5 of Table 8 (for the corresponding justification see text in Section 8.3); with Eq. (30d) and the now known values for K_I and $K_{I/O}$, that for $K_{I/st}$ may be calculated (column 6). All error limits in this table correspond to 3-times the standard deviation (3σ); they were calculated according to the error propagation after Gauss.

[b] These values were calculated via Eq. (27) with $K_{I/O}$ and %Cu(arm)(PMEA)$_{op}$.

[c] The values for %Cu(arm)(PMEA)$_{st}$ follow from the difference %Cu(arm)(PMEA)$_{int/tot}$ − %Cu(arm)(PMEA)$_{cl/O}$ (cf. Eqs. (30b and 30c)); %Cu(arm)(PMEA)$_{st}$ may also be calculated via Eq. (28) with $K_{I/st}$ and %C(arm)(PMEA)$_{op}$. The results are the same for both calculation methods (aside from possible differences in the last digit due to differences in rounding) yet the error limits (which are given in parenthesis) are understandably larger for the second method.

interaction between bpy or phen and an adenine residue. The actual formation degrees of the intramolecular stacks in Cu(bpy)(5′-AMP) and Cu(phen)(5′-AMP) are 81 (±4)% and 90 (±2)%, respectively [39], and, in fact, these values are rather similar to those observed for Cu(bpy)(PMEA) and Cu(phen)(PMEA) (see Table 9).

9. Comparison of properties of PMEA with those of 5′-AMP

The dianion of 9-[2-(phosphonomethoxy)ethyl]adenine ($PMEA^{2-}$) is a fascinating ligand which resembles in many respects adenosine 5′-monophosphate ($5'\text{-}AMP^{2-}$; see Fig. 1). Indeed, those properties which depend only on the qualities of the adenine moiety, such as H-bonding, stacking interactions, or metal ion coordination, as long as no sites different from those of the adenine residue are additionally involved, are expected to be very similar or even identical. In fact, that the adenine residue of PMEA may form adenosine-type complexes has been shown by the formation of monoprotonated $M(H{\cdot}PMEA)^{-}$ species [7] in which the metal ion is mainly located at the adenine residue and the proton at the phosphonate group.

The lengths of the D-ribose 5-monophosphate residue and of the (phosphonomethoxy)ethane residue are also very similar; thus, a metal ion coordinated at the phosphate group of $5'\text{-}AMP^{2-}$ or at the phosphonate group of $PMEA^{2-}$ is placed at about the same distance from the adenine moiety; in other words, the 'open' isomers of the corresponding complexes (see Section 5) are structurally quite alike. However, there are also crucial differences between $5'\text{-}AMP^{2-}$ and $PMEA^{2-}$ with regard to the structures of metal ion complexes formed: with $5'\text{-}AMP^{2-}$ alkaline earth ions only bind to the phosphate group, while divalent 3d ions and Zn^{2+} or Cd^{2+} form macrochelates involving N-7 of the adenine moiety [20,22]. In contrast, with $PMEA^{2-}$ all the metal ions studied interact not only with the phosphonate group but to a remarkable extent also with the neighboring ether O-atom, forming five-membered chelates as expressed in equilibrium (1) (Section 5). The adenine residue of $PMEA^{2-}$ is only exceptionally involved in metal ion binding, as e.g. with Cu^{2+} and, if so, most probably via N-3 (see Section 6).

In other words, all enhanced complex stabilities observed so far for M(AMP) complexes could always be attributed to an interaction with N-7 [20,22], while the enhanced complex stabilities of the M(PMEA) complexes have to be attributed mainly to the interaction with the ether O-atom [7]. This means that the structures of the complexes having only a phosphate or phosphonate metal ion interaction are similar, yet those isomers which contain chelates are very different for AMP^{2-} and $PMEA^{2-}$. At this point it may be recalled that the ether O-atom is crucial for the biological activity of PMEA, e.g. its antiviral action [4,43].

As said above, the stacking properties of 5′-AMP and PMEA are expected to be similar. In accord herewith, the mixed ligand species Cu(arm)(5′-AMP) and Cu(arm)(PMEA), in which stacking is dominating, appear to be quite alike (Section 8), while the binary M(5′-AMP) and M(PMEA) complexes differ considerably in their structures owing to the participation of the ether oxygen in the complex forming properties of $PMEA^{2-}$. However, there is the possibility that the ether

oxygen also has a bearing in mixed ligand complexes: with metal ions such as Zn^{2+} [42], which prefer an octahedral, square-pyramidal or tetrahedral coordination sphere, it would be sterically possible in mixed ligand complexes of the kind described (Section 8) to have ether O-coordination and stack formation at the same time. In other words, for such metal ions the structures of mixed ligand complexes containing 5′-AMP^{2-} or $PMEA^{2-}$ would be different.

In this context one may also add that the extent of stacking in the Cu(arm)(AMP) complexes containing 2′-, 3′-, or 5′-AMP^{2-} is rather different [39]. This is due to the directing properties of the phosphate group, which is located at different positions of the ribose moiety in these AMPs. Clearly, similar differences are not possible with $PMEA^{2-}$; for the latter in mixed ligand complexes stacks may only be formed in a way similar (at least in a first approximation) to those of 5′-AMP^{2-}.

10. General conclusions and outlook

Nucleotides participate in cellular metabolism as substrates or products in diverse biosynthetic pathways [6,15]. They also play a role in various regulation mechanisms [44]. With these indications in mind, the attempts to exploit artificial nucleotide analogues, including phosphonate derivatives owing to their similarity to phosphate esters, are easy to understand. Further, as in nature reactions involving nucleotides and other phosphate esters generally depend on the presence of metal ions, the metal ion binding properties of nucleotide analogues [2,7–11] and phosphonate derivatives [7–12,45] are receiving increasing attention.

In the described metal ion-binding properties of PMEA, an AMP analogue (Fig. 1), we have seen that the ether O-atom plays a significant role. It is therefore remarkable that exactly the same ether O-atom is important for the observation of any antiviral, i.e. the biological, activity of PMEA; deletion of this O-atom or replacement by other groups leads to a loss or at least a considerable reduction of the biological activity [3,4,43]. Fascinating in the present context is the finding that the only other compound with comparable biological activity, i.e. (*S*)-9-[3-hydroxy-2-(phosphonomethoxy)propyl]adenine (HPMPA) [4,43], differs from PMEA (see Fig. 1) only by the additional presence of a $-CH_2OH$ group in the chain bound to the adenine moiety, i.e., in the $-CH_2-CH(CH_2OH)-O-CH_2-PO_3^{2-}$ residue. As one might expect, preliminary studies of the complexes of $HPMPA^{2-}$ with Ca^{2+}, Cu^{2+}, or Zn^{2+} indicate [11] that their stabilities and structures are similar to those described in this review for the corresponding M(PMEA) species.

It is interesting that PMEA shows a biological activity spectrum which only partially overlaps with that of HPMPA: whereas HPMPA is exclusively active against DNA viruses [44,46], e.g., herpes viruses, adeno- and pox-viruses, PMEA is virtually inactive against some of them (adeno-, pox-viruses); yet in contrast to HPMPA, it is a potent inhibitor of retroviruses, including HIV [44,47]. It appears that PMEA, e.g., in its activity against herpes simplex virus (HSV), acts via inhibition of the viral DNA polymerase [5], while the mechanism of action of HPMPA seems to be different [5,48]. It may be added that both phosphonate derivatives, PMEA

and HPMPA, are converted in the cells to their mono- and diphosphates, which can be considered as nucleoside diphosphate and triphosphate analogues, respectively [49]. Taking into account the fact that the enzymes responsible for DNA and RNA synthesis, as well as for many other reactions involving nucleotides, are metal ion-dependent, it is conceivable that the special metal ion-binding properties of $PMEA^{2-}$ as well as of $HPMPA^{2-}$ play a role in the antiviral action of both compounds.

At this point one may recall that in active-site cavities of metalloproteins the 'solvent' polarity [32,33] and the activity of water [34] are reduced; this fact together with the results described in Section 7 regarding the alteration of structures of the complexes in dependence on the composition of the solvent should be kept in mind. For example, similar results to those summarized in Fig. 4 for Cu(PMEA) and Cu(5′-AMP) species are also to be expected for other M^{n+} ions with an affinity for imidazole- or pyridine-type nitrogens. Among the biologically relevant ions, Zn^{2+}, which is also important in nucleic acid metabolism [6,50–52], has to be placed into this category. It should be emphasized here again that with a decreasing solvent polarity the overall complex stability steadily increases despite the (unpredictable) changes in the isomeric ratios. This last-mentioned category of metal ions is distinctly different from those such as Mg^{2+} or Ca^{2+} that do not undergo a direct adenine interaction [16–18,20,22,26,53]; however, for this latter category also a decreasing solvent polarity will strongly favor the stability of the $-PO_3^{2-}/M^{2+}$ interaction [54,55].

There are two more points which finally warrant emphasis. (i) The evaluation procedures [7,8] for the quantification of isomeric equilibria between various complexes in solution, as summarized in this account, are generally applicable, i.e., to any other equilibrium system between structurally different species (or isomers) which can be defined via equilibrium constants. (ii) The differences in free energy (ΔG°) connected with the formation of low percentages of a 'chelate', e.g. of $M(PME)_{cl}$, are small: e.g., 5%, 21% or 50% $M(PME)_{cl}$ correspond to changes in log Δ (Eqs. (12), (22)) of only 0.02, 0.1 or 0.3 and regarding ΔG° to only -0.1, -0.6 or -1.7 kJ mol^{-1}, respectively [17,19]. It is evident that for an enzymic reaction a relatively small amount, e.g. 20%, of a given isomer of a complex occurring in fast equilibrium is enough to serve as substrate. In other words, here nature has a tool to achieve high selectivity by connecting various such equilibria without creating high energy barriers [56].

Acknowledgements

The competent technical assistance of Mrs. Rita Baumbusch in the preparation of the manuscript, the support of this research over the years by the Swiss National Science Foundation, and recently in part by the Swiss Federal Office for Education and Science (Human Capital and Mobility) are gratefully acknowledged. Some of the summarized research is also a part of the 'European Cooperation in the Field of Scientific and Technical Research' (COST)-D1 programme.

References

[1] (a) J.C. Martin (ed.), Nucleotide Analogues as Antiviral Agents, ACS Symposium Series 401; American Chemical Society, Washington, DC, 1989. (b) M.R. Harnden (ed.), Approaches to Antiviral Agents, VCH Verlagsgesellschaft, Weinheim, FRG, 1985. (c) H. Dvořáková and A. Holý, Collect. Czech. Chem. Commun., 58 (1993) 1419–1429. (d) K. Hartmann, J. Balzarini, J. Higgins, E. De Clercq and N.C. Pedersen, Antiviral Chem. Chemother., 5 (1994) 13–19.

[2] H. Sigel, The ambivalent properties of some base-modified nucleotides, Met. Ions Biol. Syst., 8 (1979) 125–158.

[3] A. Holý, Il Farmaco, 46 (Suppl. 1) (1991) 141–146.

[4] A. Holý, E. De Clercq and I. Votruba, ACS Symp. Ser., 401 (1989) 51–71.

[5] S.A. Foster, J. Černý and Y.-c. Cheng, J. Biol. Chem., 266 (1991) 238–244.

[6] H. Sigel and A. Sigel (eds.), Metal Ions in Biological Systems, Vol. 25, Interrelations among Metal Ions, Enzymes, and Gene Expression, M. Dekker, New York and Basel, 1989.

[7] H. Sigel, D. Chen, N.A. Corfù, F. Gregáň, A. Holý and M. Strašák, Helv. Chim. Acta, 75 (1992) 2634–2656.

[8] D. Chen, M. Bastian, F. Gregáň, A. Holý and H. Sigel, J. Chem. Soc. Dalton Trans. (1993) 1537–1546.

[9] D. Chen, F. Gregáň, A. Holý and H. Sigel, Inorg. Chem., 32 (1993) 5377–5384.

[10] M. Bastian, D. Chen, F. Gregáň, G. Liang and H. Sigel, Z. Naturforsch., 48b (1993) 1279–1287.

[11] B. Song, A. Holý and H. Sigel, Gazz. Chim. Italiana, 124 (1994) 387–392.

[12] B. Song, D. Chen, M. Bastian, R.B. Martin and H. Sigel, Helv. Chim. Acta, 77 (1994) 1738–1756.

[13] R.B. Martin and Y.H. Mariam, Met. Ions Biol. Syst., 8 (1979) 57–124.

[14] R. Tribolet and H. Sigel, Eur. J. Biochem., 163 (1987) 353–363.

[15] H. Sigel (ed.), Metal Ions in Biological Systems, Vol. 8, Nucleotides and Derivatives; Their Ligating Ambivalency, M. Dekker, New York and Basel, 1979.

[16] H. Sigel, Chem. Soc. Rev., 22 (1993) 255–267.

[17] H. Sigel, ACS Symp. Ser., 402 (1989) 159–204.

[18] H. Sigel, Eur. J. Biochem., 165 (1987) 65–72.

[19] R.B. Martin and H. Sigel, Comments Inorg. Chem., 6 (1988) 285–314.

[20] H. Sigel, S.S. Massoud and R. Tribolet, J. Am. Chem. Soc., 110 (1988) 6857–6865.

[21] (a) M.D. Reily, T.W. Hambley and L.G. Marzilli, J. Am. Chem. Soc., 110 (1988) 2999–3007. (b) M.D. Reily and L.G. Marzilli, J. Am. Chem. Soc., 108 (1986) 8299–8300.

[22] H. Sigel, S.S. Massoud and N.A. Corfù, J. Am. Chem. Soc., 116 (1994) 2958–2971.

[23] S.S. Massoud and H. Sigel, Inorg. Chem., 27 (1988) 1447–1453.

[24] H. Sigel, Coord. Chem. Rev., 122 (1993) 227–242.

[25] H. Sigel, A. Holý, C. Blindauer et al., results to be published.

[26] H. Diebler, J. Mol. Catal., 23 (1984) 209–217.

[27] (a) H. Sigel, Coord. Chem. Rev., 100 (1990) 453–539. (b) H. Sigel, Inorg. Chim. Acta, 198–200 (1992) 1–11.

[28] (a) G. Raudaschl-Sieber, H. Schöllhorn, U. Thewalt and B. Lippert, J. Am. Chem. Soc., 107 (1985) 3591–3595. (b) E. Dubler, M. Grüter-Heini, G. Hänggi, M. Knoepfel and H. Schmalle, Abstracts of the 2nd European Bioinorganic Chemistry Conference (EuroBIC II), Florence, Italy, Aug. 30–Sept. 3, 1994, p. 110.

[29] W.S. Sheldrick and B. Günther, Inorg. Chim. Acta, 152 (1988) 223–226.

[30] (a) A. Ciccarese, D.A. Clemente, A. Marzotto, M. Rosa and G. Valle, J. Inorg. Biochem., 43 (1991) 470. (b) A. Marzotto, G. Valle and D.A. Clemente, Abstracts of the 29th Int. Conf. on Coordination Chem., Lausanne, Switzerland, July 19–24, 1992, p. 72, No. P182. (c) A. Marzotto, D.A. Clemente, A. Ciccarese and G. Valle, J. Crystallogr. Spectrosc. Res., 23 (1993) 119–131.

[31] S.S. Massoud and H. Sigel, Eur. J. Biochem., 179 (1989) 451–458.

[32] (a) D.C. Rees, J. Mol. Biol., 141 (1980) 323–326. (b) G.R. Moore, FEBS Lett., 161 (1983) 171–175. (c) N.K. Rogers, G.R. Moore and M.J. E. Sternberg, J. Mol. Biol., 182 (1985) 613–616.

[33] H. Sigel, R.B. Martin, R. Tribolet, U.K. Häring and R. Malini-Balakrishnan, Eur. J. Biochem., 152

(1985) 187–193. See also the comment in the footnote on p. 258 in: M. Bastian and H. Sigel, Inorg. Chim. Acta, 178 (1990) 249–259.
[34] L. De Meis, Biochim. Biophys. Acta, 973 (1989) 333–349.
[35] (a) G. Åkerlöf and O.A. Short, J. Am. Chem. Soc., 58 (1936) 1241–1243. (b) F.E. Critchfield, J.A. Gibson, Jr. and J.L. Hall, J. Am. Chem. Soc., 75 (1953) 1991–1992. (c) G. Åkerlöf and O.A. Short, J. Am. Chem. Soc., 75 (1953) 6357.
[36] M.C.F. Magalhães and H. Sigel, J. Indian Chem. Soc., 69 (1992) 437–441.
[37] G. Liang and H. Sigel, Inorg. Chem., 29 (1990) 3631–3632.
[38] H. Sigel, Biol. Trace Elem. Res., 21 (1989) 49–59.
[39] S.S. Massoud, R. Tribolet and H. Sigel, Eur. J. Biochem., 187 (1990) 387–393.
[40] H. Sigel and R.B. Martin, Chem. Rev., 82 (1982) 385–426.
[41] (a) E.W. Wilson, Jr., M.H. Kasperian and R.B. Martin, J. Am. Chem. Soc., 92 (1970) 5365–5372. (b) H. Gampp, H. Sigel and A.D. Zuberbühler, Inorg. Chem., 21 (1982) 1190–1195.
[42] H. Sigel and R.B. Martin, Chem. Soc. Rev., 23 (1994) 83–91.
[43] A. Holý, I. Votruba, A. Merta, J. Černý, J. Veselý, J. Vlach, K. Šedivá, I. Rosenberg, M. Otmar, H. Hřebabecký, M. Trávníček, V. Vonka, R. Snoeck and E. De Clercq, Antiviral Res., 13 (1990) 295–312.
[44] A. Holý, Adv. Antiviral Drug Design, 1 (1993) 179–231.
[45] (a) T. Kiss, E. Farkas and H. Kozłowski, Inorg. Chim. Acta, 155 (1989) 281–287. (b) M. Jezowska-Bojczuk, T. Kiss, H. Kozłowski, P. Decock and J. Barycki, J. Chem. Soc. Dalton Trans. (1994) 811–817.
[46] E. De Clercq, A. Holý, I. Rosenberg, T. Sakuma, J. Balzarini and P.C. Maudgal, Nature, 323 (1986) 464–467.
[47] (a) R. Pauwels, J. Balzarini, D. Schols, M. Baba, J. Desmyter, I. Rosenberg, A. Holý and E. De Clercq, Antimicrob. Agents Chemother., 32 (1988) 1025–1030. (b) J. Balzarini, L. Naesens, P. Herdewijn, I. Rosenberg, A. Holý, R. Pauwels, M. Baba, D.G. Johns and E. De Clercq, Proc. Natl. Acad. Sci. USA, 86 (1989) 332–336.
[48] V. Vonka, E. Anisimová, J. Černý, A. Holý, I. Rosenberg and I. Votruba, Antiviral Res., 14 (1990) 117–122.
[49] I. Votruba, R. Bernaerts, T. Sakuma, E. De Clercq, A. Merta, I. Rosenberg and A. Holý, Mol. Pharmacol., 32 (1987) 524–529.
[50] F.Y.-H. Wu and C.-W. Wu, Met. Ions Biol. Syst., 15 (1983) 157–192.
[51] J.E. Coleman and D.P. Giedroc, Met. Ions Biol. Syst., 25 (1989) 171–234.
[52] (a) B.L. Vallee and D.S. Auld, Biochemistry, 29 (1990) 5647–5659. (b) B.L. Vallee, J.E. Coleman and D.S. Auld, Proc. Natl. Acad. Sci. USA, 88 (1991) 999–1003.
[53] (a) D. Pörschke, Biophys. Chem., 4 (1976) 383–394. (b) H. Diebler, F. Secco and M. Venturini, Biophys. Chem., 26 (1987) 193–205. (c) K.S. Dhathathreyan and H. Diebler, Ber. Bunsen-Ges. Phys. Chem., 95 (1991) 880–886.
[54] M. Bastian and H. Sigel, Inorg. Chim. Acta, 187 (1991) 227–237.
[55] (a) R. Tribolet, R. Malini-Balakrishnan and H. Sigel, J. Chem. Soc., Dalton Trans. (1985) 2291–2303. (b) G. Liang, N.A. Corfù and H. Sigel, Z. Naturforsch., 44b (1989) 538–542.
[56] H. Sigel, Pure Appl. Chem., 61 (1989) 923–932.